Table 1. Clinical Characteristics of 146 Patients Whose Liver and Blood Samples Were Analyzed by RT-PCR

	Major (MA)				Minor (MI)		
Clinical Category	Major ISG Up (MAu)		Major ISG Down (MAd)				P Value
No. of patients	n = 42		n = 68		n = 36		NA
Age and sex							
Age (years)	55	(30-72)	56	(31-72)	55	(30-73)	NS
Sex (M vs. F)	27 vs. 15		34 vs. 34		19 vs. 17		NS
Treatment responses							
SVR/TR/NR	24/12/6		30/33/6		6/7/23*		MAu vs. MI < 0.0001, MAd vs. MI < 0.0001
IL28B genotype (TT vs. TG+GG)	TT		TT		TG/GG (31/5)		NA
Liver factors							
F stage (1/2/3/4)	14/13/11/4		30/20/11/7		14/8/10/4		NS
A grade (A0-1 vs. A2-3)	16 vs. 26		37 vs. 31		20 vs. 16		NS
ISGs (Mx1, IFI44, IFIT1)	3.83*	(2.14-9.48)	1.30*	(0.36-2.08)	5.52*	(0.86-17.3)	MAu vs. MAd < 0.0001, MAu vs. MI < 0.0001, MAd vs. MI < 0.0001
IL28A/B	41.3*	(4-151)	11.7*	(1-53)	22.7*	(3-93)	MAu vs. MAd < 0.0001, MAu vs. MI = 0.0004, MAd vs. MI = 0.031
Blood factors							
ISGs (Mx1, IFI44, IFIT1)	11.1*	(2.78-24.9)	4.76	(0.41-20.6)	5.64	(0.71-2.8)	MAu vs. MAd < 0.0001, MAu vs. MI < 0.0001
IL28A/B	1.6	(0.1-7.7)	1.3	(0.2-6.4)	1.3	(0.3-3.6)	NS
Laboratory parameters							
HCV-RNA (KIU/mL)	2,430	(160-5,000)	2,692	(140-5,000)	1,854*	(126-5,000)	MAd vs. MI = 0.017
BMI (kg/m2)	24	(18.7-31.9)	24	(16.3-34.7)	22.8	(19.1-30.5)	NS
AST (IU/L)	86*	(22-258)	54	(18-192)	64	(21-178)	MAu vs. MAd = 0.0008
ALT (IU/L)	112*	(17-376)	75	(16-345)	79	(18-236)	MAu vs. MAd = 0.023
γ-GTP (IU/L)	99*	(21-392)	47	(4-367)	74	(20-298)	MAu vs. MAd = 0.0003
WBC (/mm3)	4,761	(2,100-8,100)	4,982	(2,800-9,100)	4,823	(2,500-8,200)	NS
Hb (g/dL)	14.1	(11.4-16.7)	14.1	(9.3-16.9)	13.9	(11.2-16.4)	NS
PLT (× 104/mm3)	15.2	(9.2-27.8)	16.8	(7-39.4)	16.3	(9-27.8)	NS
TG (mg/dL)	112	(42-248)	102	(42-260)	136*	(30-323)	MAd vs. MI = 0.02
T-Chol (mg/dL)	162	(90-221)	169	(107-229)	167	(81-237)	NS
LDL-Chol (mg/dL)	77	(36-123)	83*	(42-134)	72	(29-107)	MAd vs. MI = 0.04
HDL-Chol (mg/dL)	40	(18-67)	43	(27-71)	47*	(27-82)	NS
Viral factors							
ISDR mutations ≦ 1 vs. ≧ 2	23 vs. 19*		51 vs. 17		26 vs. 10		MAu vs. MAd = 0.02
Core aa 70 (wild-type vs. mutant)	24 vs. 18		42 vs. 22		16 vs. 20*		MAd vs. MI = 0.02

*$P < 0.05$.

Abbreviations: BMI, body mass index; ALT, alanine aminotransferase; WBC, leukocytes; Hb, hemoglobin; PLT, platelets; TG, triglycerides; T-chol, total cholesterol; LDL-chol, low density lipoprotein cholesterol; HDL-chol, high density lipoprotein cholesterol; NA, not applicable; NS, not significant.

tetratricopeptide repeats 1 [IFIT1], and myxovirus (influenza virus) resistance [Mx1]) with a high dynamic range, comparable relative expression, and good predictive performance.[6] Mean values of the three ISGs detected by real-time detection polymerase chain reaction (RTD-PCR) in 168 liver tissue samples (Supporting Table 1) showed a significant up-regulation of their expression in nonresponder or treatment-resistant IL28B MI (TG/GG; rs8099917) patients, compared to responder (SVR+TR) or treatment-sensitive IL28B MA (TT; rs8099917) patients, as reported previously (Fig. 1A and Supporting Fig. 1A).[6] However, ISG expression in 146 blood samples (Table 1) showed no difference between responders and nonresponders or the IL28B major and minor genotypes (Fig. 1B and Supporting Fig. 1B). To explore these findings further, gene expression profiling using Affymetrix GeneChips was performed on liver and blood samples from 85 patients (Supporting Tables 2 and 3), and the expression of 37 representative ISGs[6] was compared (Fig. 1C-E). MA patients were divided into two groups according to their ISG expression pattern in the liver: MAu and MAd. MI patients expressed ISGs at a higher level than MAu patients. Interestingly, ISG expression in MA patients showed a similar expression pattern in liver and blood, and ISGs were up-regulated in MAu patients and down-regulated in the MAd patients. However, MI patients showed a different ISG expression pattern in liver and blood, where ISGs were up-regulated in the liver, but down-regulated in the blood (Fig. 1C). The correlation of the mean values of the three ISGs (IFI44, IFIT1, and Mx1) between liver and blood from 146 patients demonstrated a significant correlation between values in MA patients (Fig. 1D), whereas no correlation was observed in MI patients (Fig. 1E). Interestingly, ISG expression correlated significantly between liver and blood of responders, but not of nonresponders, in MA and MI patients (Supporting Fig. 1C-F). These results indicate that the correlation of ISG expression in the liver and blood is an important predictor of treatment response.

Clinical Characteristics of IL28B MA Patients With Up- and Down-Regulated ISGs and IL28B MI Patients. From the expression pattern of ISGs and mean values of the three ISGs (IFI44, IFIT1, and Mx1), we could use receiver operating characteristic curve analysis to set a threshold of 2.1-fold to differentiate MAu and MAd patients. Following this criterion, 42 MAu, 68 MAd, and 36 MI patients (total, 146) were grouped (Table 1). Hepatic ISG expression was highest in MI patients, whereas blood ISG expression was highest in MAu patients. Conversely, hepatic IL28A/B (IFN-λ2/3) expression was highest in MAu patients, whereas blood IL28A/B expression showed no difference among the three groups. Serum alanine aminotransferase (ALT), aspartate aminotransferase (AST), and gamma-glutamyl transpeptidase (GGT) levels were significantly higher in MAu patients than in MAd patients. Interestingly, serum ALT levels were significantly correlated with ISG expression in MA patients, but not in MI patients (Supporting Fig. 2E,F).

Gene expression profiling in peripheral immune cells showed the presence of active inflammation in MAu patients, whereas the inactive or remissive phase of inflammation was observed in MAd patients. In contrast, monophasic and intermediate inflammation existed in MI patients (Supporting Fig. 3).

Reduced Number of Immune Cells in the Liver Lobules of IL28B MI Patients. To examine the discordant expression of ISGs in liver and blood of MI patients, we performed LCM to collect cells in liver lobules (CLLs) and cells in portal areas (CPAs) separately from each of five liver biopsied samples from MAu, MAd, and MI patients (Fig. 2A). Interestingly, the ISG expression pattern in CLLs from MA patients was similar to that of CPAs, and ISGs were up-regulated in MAu patients and down-regulated in MAd patients. ISG expression in CLLs from the MI patients was different to that in CPAs, and ISGs were up-regulated in CLLs, but down-regulated in CPAs (Fig. 2A). We hypothesized that the discordance of ISG expression between CLLs and CPAs in MI patients might be the result of the lower number of immune cells that infiltrated the liver lobules of these patients. To prove this hypothesis, immunohistochemical (IHC) staining was performed (Fig. 2B). IHC staining showed that IFI44 was strongly expressed in the cytoplasm and nucleus of CLLs from MI patients, whereas it was intermediately expressed in MAu patients and weakly expressed in MAd patients. Interestingly, IFI44 was strongly expressed in CPAs of MAu patients and weakly expressed in CPAs of MAd patients, showing a correlation between expression in CLLs and CPAs of MA patients, whereas ILI44 expression was relatively weak in CPAs, compared with CLLs, in MI patients (Fig. 2B). In the same section of the specimens, there were less CD163-positive monocytes and macrophages in MI patients than in MAu and MAd patients. Similarly, there were fewer CD8-positive T cells in MI patients than in MAu and MAd patients (Fig. 2B). Semiquantitative evaluation of CD163- and CD8-positive lymphocytes in liver lobules showed a significantly lower number of cells in

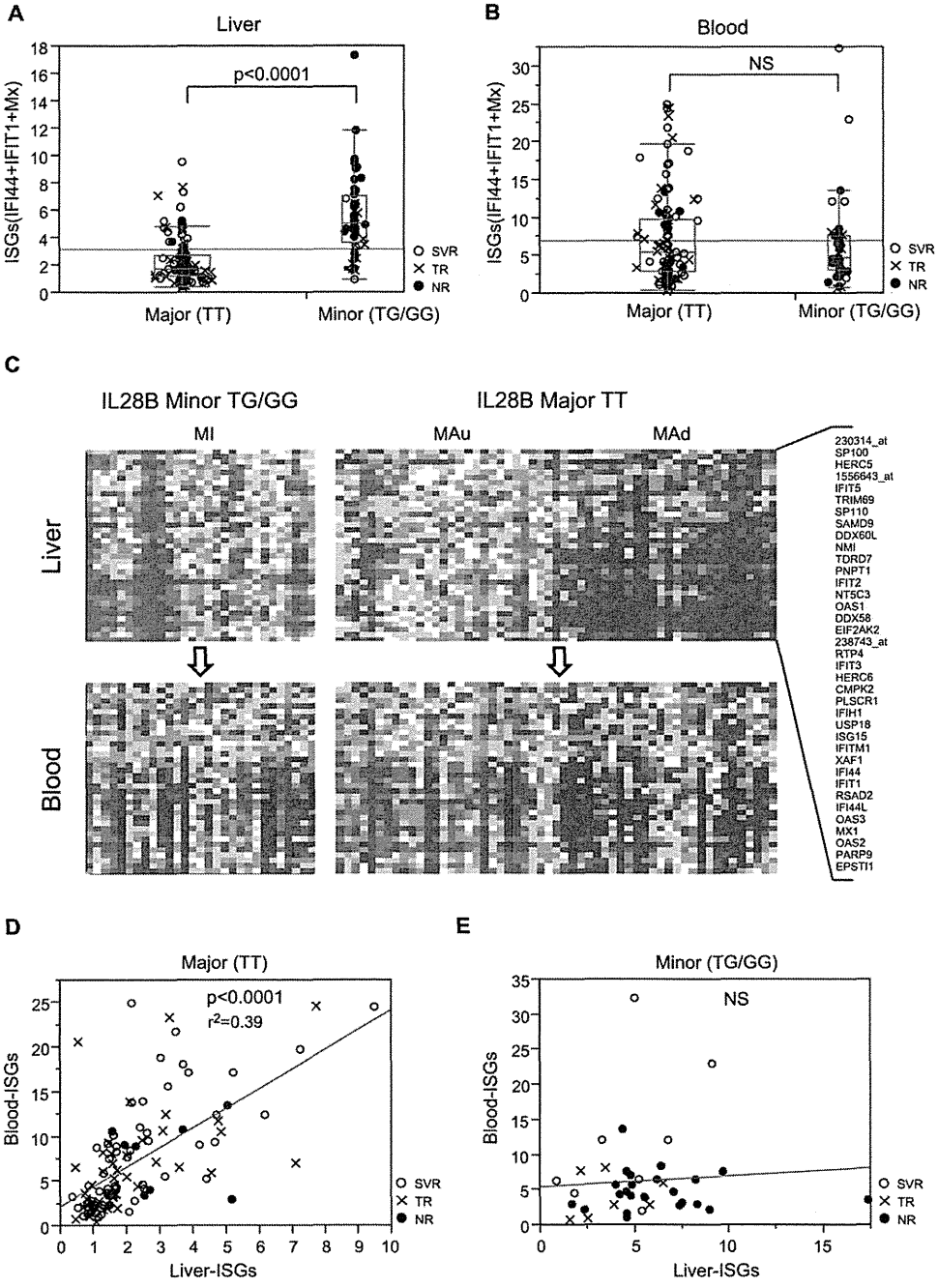

Fig. 1. Comparison of ISG expression in liver and blood of patients with different IL28B genotypes. (A and B) RTD-PCR results of mean ISG expression (IFI44-IFIT1+Mx1) in liver (A) and blood (B) of IL28B major (MAu/Mad) and minor (MI) genotype patients. (C) One-way hierarchical clustering analysis of 85 patients using 37 representative ISGs derived from liver (upper) and blood (lower). (D and E) Correlation of mean ISG expression (IFI44-IFIT1+Mx1) in liver and blood of IL28B major (MA; D) and minor (MI; E) genotype patients.

MI patients than in MAu and MAd patients (Supporting Fig. 4A,B). To support these findings, we examined the expression of 24 surface markers of immune cells in CLL, including dendritic cells (DCs), natural killer (NK) cells, macrophages, T cells, B cells, and granulocytes (Supporting Fig. 5A). The expression of immune cell-surface markers was repressed in MI patients, compared to MAu and MAd patients. Furthermore, whole-liver expression profiling in 85 patients showed the reduced expression of these surface markers in MI patients, compared to MAu and MAd patients (Supporting Fig. 5B). These results indicated that fewer immune cells had infiltrated the liver lobules of MI patients.

In addition to these findings, various chemokines, such as CC chemokine ligand (CCL)19, CCL21, CCL5, and chemokine (C-X-C motif) ligand (CXCL)13, which are important regulators for the recruitment of DCs, NK cells, T cells, and B cells in the liver, were significantly down-regulated in MI patients, compared to MAd and MAu patients (Supporting Fig. 4C-F).

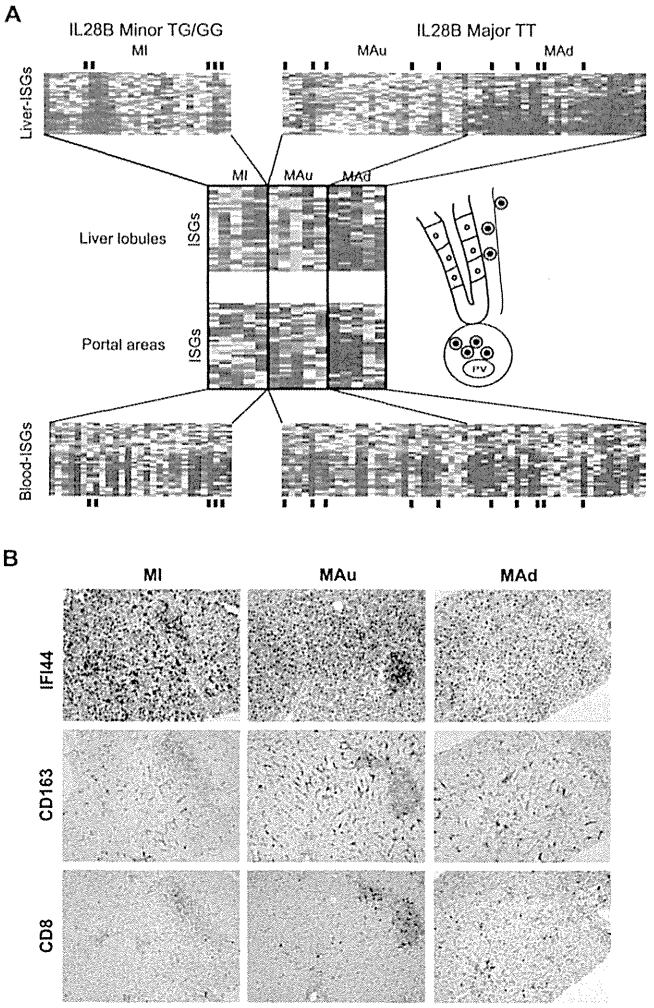

Fig. 2. LCM and IHC staining of biopsied liver specimens. (A) Comparison of the ISG expression pattern of whole liver (upper), CLLs (upper middle), CPAs (lower middle), and blood (bottom). CLLs and CPAs were obtained from 5 MI, MAu, and MAd patients, who are indicated by small black bars. (B) IHC staining of IFI44, CD163, and CD8 in MI, MAu, and MAd patients.

Hepatic ISG Expression Is Significantly Correlated With IL28A/B, but not IFN-α or IFN-β. The lower number of immune cells in the liver lobules of MI patients implies that reduced levels of IFN are produced from DCs, macrophages, and so on. These findings prompted us to examine the relationship between hepatic ISGs and IFN-α, IFN-β, IL29/IFN-λ1, and IL28A/B in CHC patients. Hepatic ISG expression was significantly correlated with IL28A/B, but not IFN-β (Fig. 3A-C) or IFN-α (data not shown) in MAu, MAd, and MI patients. Expression of IL29 was correlated with hepatic ISG expression only in MAu patients. These results indicate that hepatic ISGs would be mainly induced by IL28A/B in CHC patients. Interestingly, the correlation between hepatic ISGs and IL28A/B was strongest in MA patients ($P < 0.0001$ in MAu; $P = 0.0006$ in MAd), whereas rather a weak correlation was observed in MI patients ($P = 0.015$). Moreover, the ratio of hepatic ISGs to IL28A/B was larger in MI patients than in MA patients (S = 0.061 in MI; S = 0.028 in MAu; S = 0.020 in MAd), suggesting the presence of additional factors that can induce expression of ISGs in MI patients. Therefore, we evaluated the expression of the recently discovered IFN-λ4 in MI patients. Interestingly, there was a significant correlation between hepatic ISG and IFN-λ4 expression ($P = 0.0003$; Fig. 3C).

Wingless-Related MMTV Integration Site 5A and Its Receptor, Frizzled Receptor 5, Are Significantly Up-Regulated in the Liver of Patients With the IL28B MI. IFN-λ4 is a promising factor to induce ISG expression in MI patients,[8] and the functional relevance of IFN-λ4 for the pathogenesis of CHC is under investigation. We searched for other factors that could induce ISG expression in MI patients. A closer observation of gene expression profiling in CLLs obtained by LCM demonstrated that WNT signaling was specifically up-regulated in MI patients

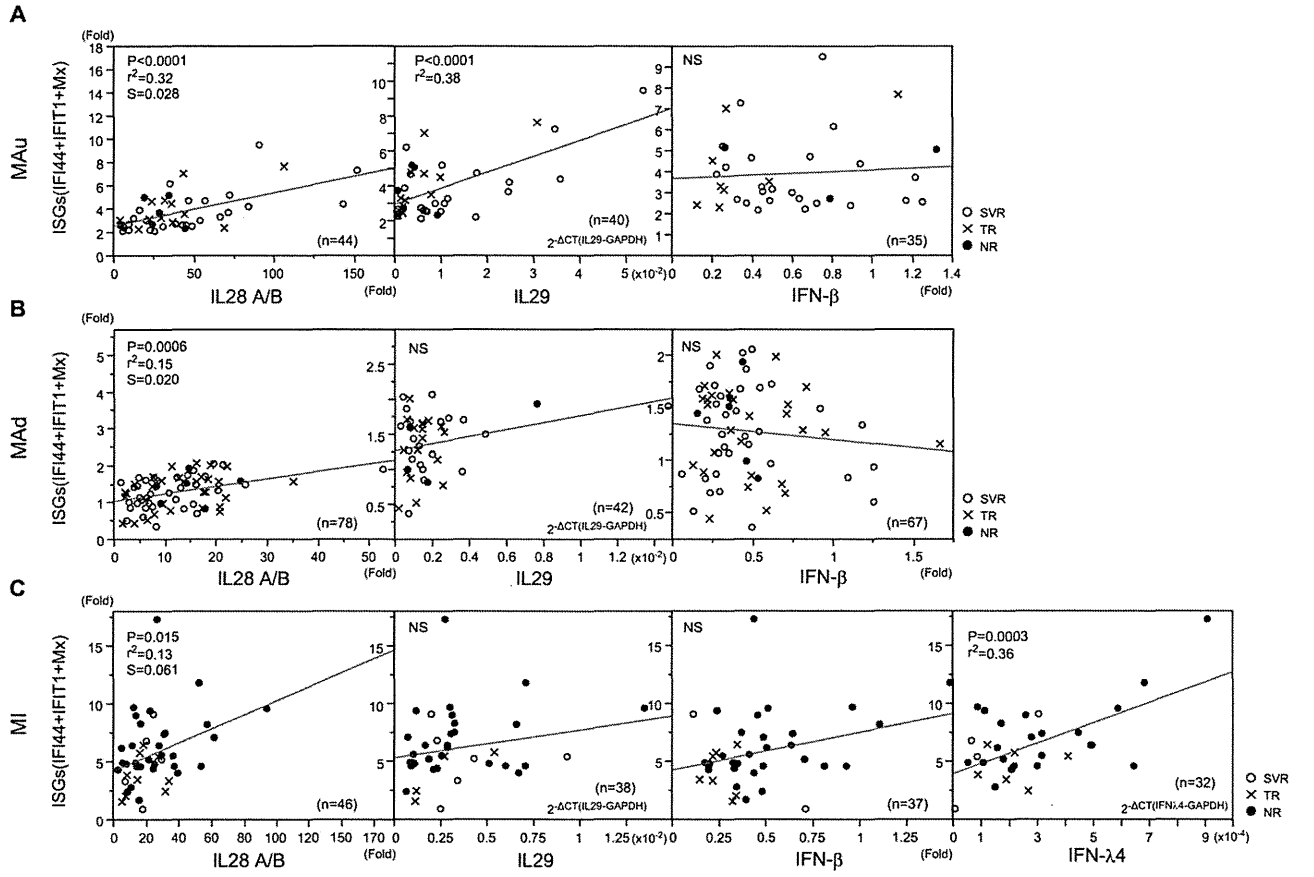

Fig. 3. Correlation analysis of hepatic ISGs and IL28A/B, IL29, IFN-β, and IFN-λ4. Correlation of mean ISG (IFI44+IFIT1+Mx1) and IL28A/B, IL29, IFN-β, and IFN-λ4 expression was evaluated in MAu (A), MAd (B), and MI (C) patients. [Color figure can be viewed in the online issue, which is available at wileyonlinelibrary.com.]

(Supporting Fig. 6). Further observation enabled us to identify that the WNT ligand, wingless-related MMTV integration site 5A (WNT5A), and its receptor, frizzled receptor 5 (FZD5), were up-regulated in MI patients. RTD-PCR results on 168 liver-biopsied samples confirmed the significant up-regulation of WNT5A and FZD5 in MI patients, compared to MAu and MAd patients (Fig. 4A,B). Interestingly, WNT5A expression was negatively correlated with chemokine expression (Supporting Fig. 7). IHC staining showed up-regulation of FZD5 in liver lobules of MI patients, but not in MAu or MAd patients (Fig. 4C). WNT5A expression was significantly correlated with hepatic ISG expression in MI and MAd patients (Fig. 4D). Interestingly, we found a weak, but significant, correlation between WNT5A and IFN-λ4 expression in MI patients (Fig. 4E).

WNT5A Induces ISG Expression, but Stimulates HCV Replication in Huh-7 Cells. To examine the functional relevance of up-regulated expression of WNT5A in MI patients, we first evaluated expression levels of WNT5A and ISGs (2′-5′-oligoadenylate synthetase 2 [OAS2], Mx1, IFI44, and IFIT1) in two immortalized human hepatocyte cell lines, THLE-5b and TTNT cells (Supporting Materials and Methods), and one human hepatoma cell line, Huh-7 cells (Supporting Fig. 8A,B). WNT5A was moderately expressed in THLE-5b and TTNT cells, whereas its expression in Huh-7 cells was minimal. Interestingly, ISG expression in these cells correlated well with expression of WNT5A (Supporting Fig. 8B). Small interfering RNA (siRNA) to WNT5A efficiently repressed WNT5A expression to ~20% of the control in THLE-5b cells, and in this condition, ISG expression was significantly decreased to 30%-50% of the control (Supporting Fig. 8C). Conversely, transduction of WNT5A using a lentivirus expression system in Huh-7 cells significantly increased OAS2 expression (Supporting Fig. 8D), as well as Mx1 and IFIT1 expression (data not shown), in the presence and absence of HCV infection. Surprisingly, HCV replication, as determined using Gaussia luciferase activity, increased in WNT5A-transduced cells (Supporting Fig. 8E). Furthermore, WNT5A-transduced cells supported more HCV replication than

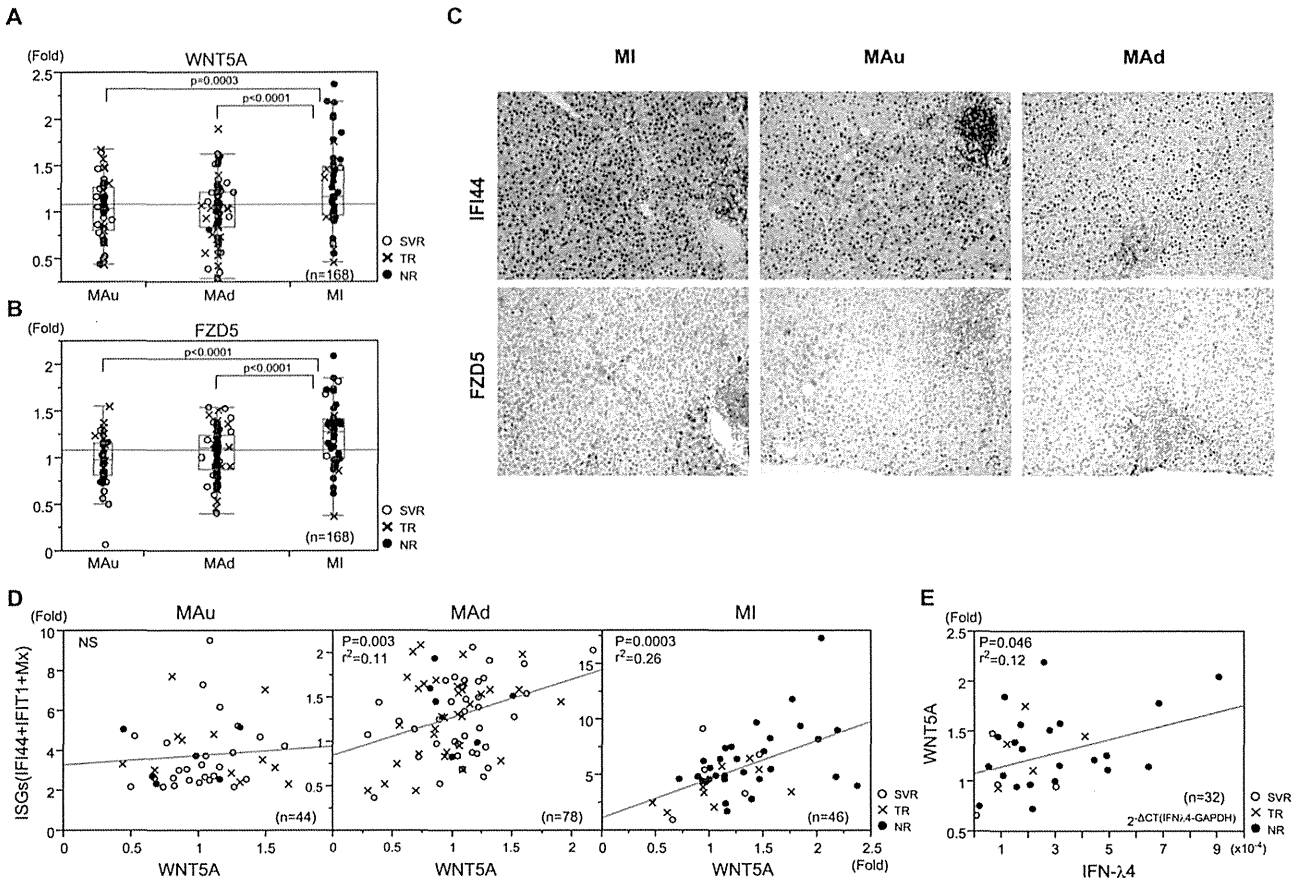

Fig. 4. WNT5A and FZD5 are up-regulated in IL28B MI patients. (A) RTD-PCR results of WNT5A expression in liver of MAu, MAd, and MI patients. (B) RTD-PCR results of FZD5 expression in liver of MAu, MAd, and MI patients. (C) IHC staining of IFI44 and FZD5 expression in liver of MAu, MAd, and MI patients. (D) Correlation of mean ISG (IFI44+IFIT1+Mx1) and WNT5A expression in liver of MAu, MAd, and MI patients. (E) Correlation of WNT5A and IFN-λ4 expression in liver of MI patients.

nontransduced cells under IFN treatment (Supporting Fig. 8F).

WNT5A-FZD5 Signaling Induces the Expression of the Stress Granule Protein, GTPase-Activating Protein (SH3 Domain)-Binding Protein 1, Which Supports HCV Replication. These findings were further confirmed by using Huh-7 cells that were continuously infected with Japanese fulminant hepatitis type 1 (JFH-1; Huh7-JFH1), which is a genotype 2a HCV isolate.[9] Interestingly, expression of WNT5A in Huh7-JFH1 cells was significantly up-regulated, compared with uninfected Huh-7 cells, and showed an equivalent expression level with THLE-5b cells (Fig. 5A). siRNA to WNT5A efficiently repressed WNT5A expression to ~20% of the control, and in this condition, ISG expression (IFI44 was not expressed in Huh-7 cells), HCV RNA, and infectivity were repressed to 25%-65%, 60%, and 40% of the control, respectively (Fig. 5B and Supporting Fig. 9A). Interestingly, CXCL13 expression was significantly increased in this condition. We evaluated the expression of GTPase-activating protein (SH3 domain)-binding protein 1 (G3BP1), a recently recognized stress granule (SG) protein that supports HCV infection and replication.[10] Expression of G3BP1 was repressed to 60% of the control by knocking down WNT5A. Conversely, overexpression of WNT5A in Huh7-JFH1 cells significantly decreased CXCL13 expression and increased HCV RNA, infectivity, and G3BP1 expression (Fig. 5C and Supporting Fig. 9B). A recent report demonstrated that G3BP1 is a disheveled (DVL)-associated protein that regulates WNT signaling downstream of the FZD receptor.[11] Knocking down FZD5 in Huh7-JFH1 cells significantly reduced the expression of DVL1-3, G3BP1, Mx1, and IFIT1 as well as HCV infectivity (Supporting Fig. 9C,D). Interestingly, G3BP1 expression was significantly up-regulated in liver of MI patients (Fig. 5D). Furthermore, G3BP1 expression was significantly correlated with WNT5A expression in liver of the CHC patients (Fig. 5E). More dramatically, a strong correlation was observed between expression of FZD5 and G3BP1 in liver of CHC patients (Fig. 5F).

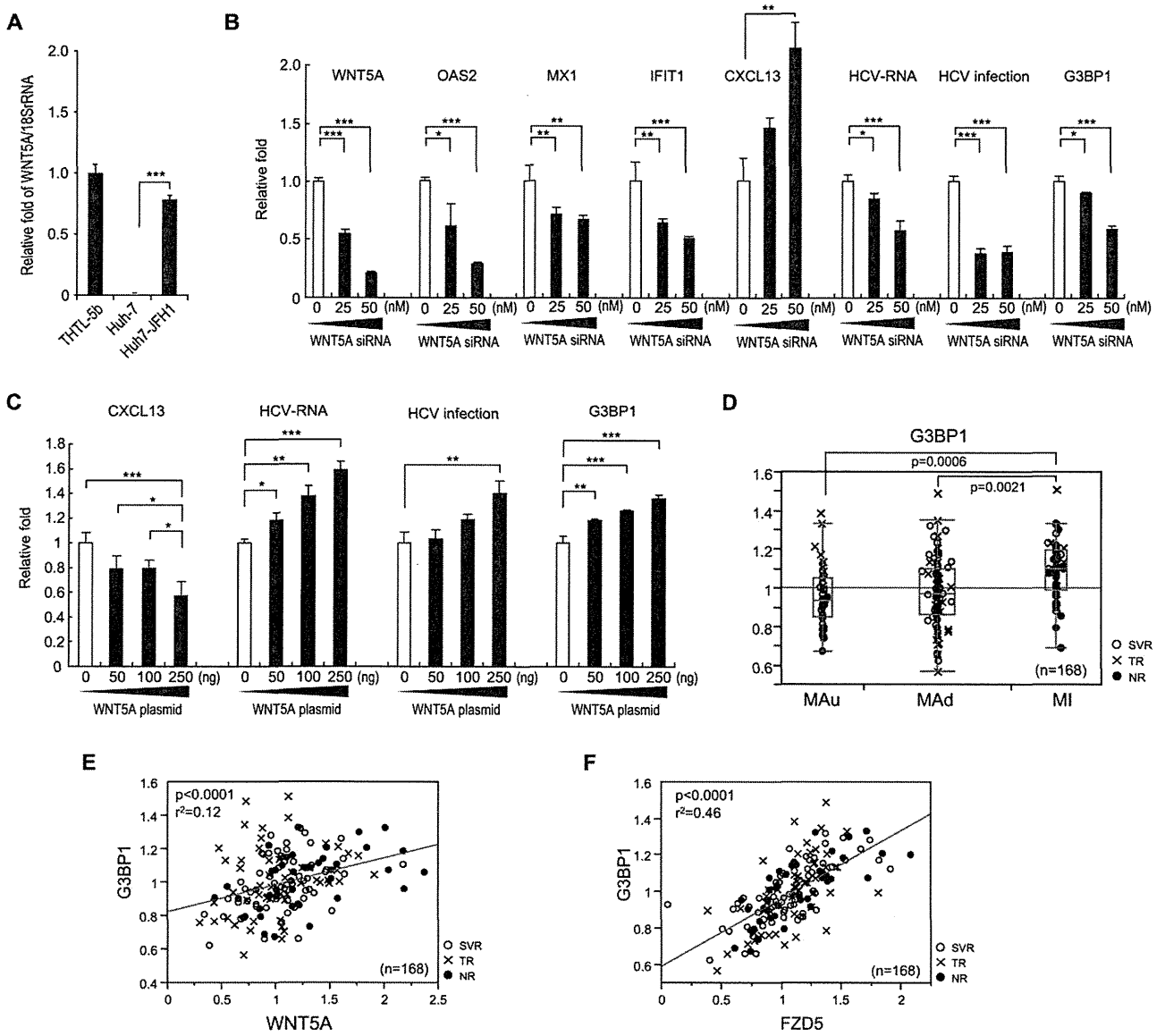

Fig. 5. Relationship between WNT5A and FZD5 signaling and the SG protein, G3BP1. (A) WNT5A expression in THLE-5b, Huh-7, and Huh7-JFH1 cells. (B) Knocking down WNT5A and changes of OAS2, Mx1, IFIT1, CXCL13, and G3BP1 expression, HCV RNA, and infectivity in Huh7-JFH1 cells. (C) Overexpression of WNT5A after transfection with pCMV-WNT5A and decrease in CXCL13 expression and increase in HCV RNA, infectivity, and G3BP1 expression. (A-C) Experiments were performed in duplicate and repeated three times (n = 6). Values are the means ± standard error. $*P < 0.05$; $**P < 0.01$; $***P < 0.005$. (D) RTD-PCR results for G3BP1 expression in liver of MAu, MAd, and MI patients. (E) Correlation of WNT5A and G3BP1 expression in the liver. (F) Correlation of FZD5 and G3BP1 expression in the liver. [Color figure can be viewed in the online issue, which is available at wileyonlinelibrary.com.]

Discussion

The underlying mechanism for the association of the IL28B genotype with treatment responses to IFN-based therapy for HCV has not yet been clarified. We and others have shown that pretreatment up-regulation of hepatic ISGs was associated with an unfavorable treatment outcome[7,12,13] and was closely related to treatment-resistant MI IL28B, compared with treatment-sensitive MA IL28B.[6]

By comparing ISG expression in liver and blood, we found that their expression was correlated in MA patients, but not in MI patients. LCM analysis of ISG expression in CLLs and CPAs showed the loss of the correlation between CLLs and CPAs in MI patients (Fig. 2A). This might be the result of the impaired migration of immune cells into liver lobules that was demonstrated by decreased expression of immune cell-surface markers in CLLs by LCM (Supporting Fig. 5A) and IHC staining (Fig. 2B). Lymphocyte accumulation in the portal area (portal-tract-associated lymphoid tissue; PALT) might be involved in extravasation of lymphocytes from vessels in the portal area, but

others demonstrated that DCs appeared in the sinusoidal wall and passed through the space of Disse to PALT, where the draining lymphatic duct is located.[14] There should be an active movement of immune cells between liver lobules and PALT, as reflected by the correlation of ISG expression in CLLs and CPAs in the MA patients of this study.

ISGs were reportedly up-regulated in hepatocytes of treatment-resistant IL28B genotype patients, but were up-regulated in Kupffer cells of treatment-sensitive genotype patients.[15] Our results confirmed these findings; however, we also showed that expression of various immune cell-surface markers, such as those on DCs, NK cells, macrophages, T cells, B cells, and granulocytes, was lower in MI than in MA patients (Supporting Fig. 5). In addition, we showed that expression of various chemokines was also repressed in MI patients, compared to MA patients (Supporting Fig. 4C-F).

Up-regulation of pretreatment chemokine (C-X-C motif) ligand 10/interferon-gamma-induced protein 10 (CXCL10/IP-10) serum levels is also associated with an unfavorable treatment outcome.[16] CXCL10 expression in the liver was significantly correlated with hepatic ISG expression and was higher in nonresponders than in responders (Supporting Fig. 10). Our results support the usefulness of serum CXCL10 for prediction of treatment outcome. Chemokine (C-X-C motif) receptor 3 (CXCR3) expression, a receptor for CXCL10, was inversely correlated with hepatic ISG expression and was significantly lower in MI than in MA patients (Supporting Fig. 10).

The lower number of immune cells in the liver lobules of MI patients would imply the reduced production of IFN from DCs, macrophages, and so on. Correlation analysis showed that hepatic ISGs were mainly associated with type III IFNs (IL28A/B and IL29), but not type I IFNs (IFN-α or IFN-β), although a significant association with IL29 was only observed in MA patients with up-regulated ISGs. This might be related to the high serum ALT levels in MAu patients (Fig. 3). Closer examination of hepatic ISGs and IL28A/B suggested that factors other than IL28A/B might regulate ISG expression in MI patients. During the preparation of this study, IFN-λ4 was newly identified to be expressed in hepatocytes from treatment-resistant IL28B genotype patients.[8] Interestingly, we found a significant correlation between hepatic ISGs and IFN-λ4 in MI patients (Fig. 3C). Moreover, a closer examination of gene expression profiling in MI patients enabled us to detect up-regulation of the noncanonical WNT ligand, WNT5A. RTD-PCR analysis of 168 patients confirmed up-regulation of WNT5A and its receptor, FZD5, in MI patients. Importantly, WNT5A expression was significantly correlated with hepatic ISG expression in MI patients. A recent report showed that WNT5A induces expression of ISGs, increases sensitivity of keratinocytes to IFN-α,[17] and might be involved in the immune response to influenza virus infection.[18] Therefore, we examined the role of WNT5A in hepatocytes. Interestingly, expression of WNT5A and ISGs was well correlated, and knocking down WNT5A using siRNA reduced expression of ISGs in THLE-5b cells (Supporting Fig. 8). Conversely, transduction of Huh-7 cells with WNT5A using a lentivirus system increased expression of ISGs. Despite the increase in ISG expression, WNT5A did not suppress HCV replication, but rather increased it in Huh-7 cells (Supporting Fig. 8). These results were also confirmed by using Huh-7 cells continuously infected with JFH-1. By knocking down or overexpressing WNT5A in Huh7-JFH1 cells, we showed that HCV-RNA was positively regulated by WNT5A (Fig. 5B,C).

WNT5A and its receptor, FZD5, mediate noncanonical WNT signaling, such as planar cell polarity and the WNT-Ca^{2+}-signaling pathway through G proteins. WNT5A reportedly inhibits B- and T-cell development by counteracting canonical WNT signaling.[19] We found that G3BP1, an SG assembly factor, was up-regulated by WNT5A (Fig. 5C). SGs were reportedly formed by endoplasmic reticulum stress, followed by HCV infection, and localized around lipid droplets with HCV replication complexes.[10] G3BP1 contributes to SG formation and increases HCV replication and infection in Huh-7 cells.[10] Moreover, a recent report demonstrated that G3BP1 is a DVL-associated protein that regulates WNT signaling downstream of the FZD receptor.[11] In this study, repression of WNT5A or FZD5 significantly reduced expression of DVL1-3, G3BP1, Mx1, and IFIT1 as well as HCV infectivity in Huh7-JFH1 cells (Fig. 5 and Supporting Fig. 9).

Importantly, we found a significant correlation between WNT5A and G3BP1 expression in liver tissue samples (Fig. 5E). We also found a significant correlation between FZD5 and G3BP1 expression in liver tissue samples (Fig. 5F). Thus, up-regulated noncanonical WNT5A-FZD5 signaling participates in the induction of ISG expression, but preserves HCV replication and infection in hepatocytes by increasing levels of the SG protein, G3BP1. These findings may explain the pathophysiological state of the treatment-resistant phenotype in MI patients.

In this study, we demonstrated impaired immune cell infiltration of the liver in treatment-resistant IL28B genotype patients, and we also demonstrated

that up-regulation of hepatic ISGs in treatment-resistant IL28B genotype patients was mediated by multiple factors, including IL28A/B, IFN-λ4, and WNT5A. We found a significant negative correlation between WNT5A and various chemokines in liver of CHC patients (Supporting Fig. 7). Interestingly, WNT5A directly repressed one of these chemokines, CXCL13, a B-lymphocyte chemoattractant, in HCV-infected hepatocytes. These results indicate that loss of immune cells from the liver may be associated with the induction of other inflammatory factors, such as WNT5A, in MI patients, although we did not identify which cells express WNT5A. Further studies are needed to explore their functional relevance in the pathogenesis of CHC.

Acknowledgment: The authors thank Mina Nishiyama for her technical assistance.

References

1. Fried MW, Shiffman ML, Reddy KR, Smith C, Marinos G, Goncales FL, Jr., et al. Peginterferon alfa-2a plus ribavirin for chronic hepatitis C virus infection. N Engl J Med 2002;347:975-982.
2. Zeuzem S, Andreone P, Pol S, Lawitz E, Diago M, Roberts S, et al. Telaprevir for retreatment of HCV infection. N Engl J Med 2011;364:2417-2428.
3. Ge D, Fellay J, Thompson AJ, Simon JS, Shianna KV, Urban TJ, et al. Genetic variation in IL28B predicts hepatitis C treatment-induced viral clearance. Nature 2009;461:399-401.
4. Suppiah V, Moldovan M, Ahlenstiel G, Berg T, Weltman M, Abate ML, et al. IL28B is associated with response to chronic hepatitis C interferon-alpha and ribavirin therapy. Nat Genet 2009;41:1100-1104.
5. Tanaka Y, Nishida N, Sugiyama M, Kurosaki M, Matsuura K, Sakamoto N, et al. Genome-wide association of IL28B with response to pegylated interferon-alpha and ribavirin therapy for chronic hepatitis C. Nat Genet 2009;41:1105-1109.
6. Honda M, Sakai A, Yamashita T, Nakamoto Y, Mizukoshi E, Sakai Y, et al. Hepatic ISG expression is associated with genetic variation in interleukin 28B and the outcome of IFN therapy for chronic hepatitis C. Gastroenterology 2010;139:499-509.
7. Honda M, Nakamura M, Tateno M, Sakai A, Shimakami T, Shirasaki T, et al. Differential interferon signaling in liver lobule and portal area cells under treatment for chronic hepatitis C. J Hepatol 2010;53:817-826.
8. Prokunina-Olsson L, Muchmore B, Tang W, Pfeiffer RM, Park H, Dickensheets H, et al. A variant upstream of IFNL3 (IL28B) creating a new interferon gene IFNL4 is associated with impaired clearance of hepatitis C virus. Nat Genet 2013;45:164-171.
9. Wakita T, Pietschmann T, Kato T, Date T, Miyamoto M, Zhao Z, et al. Production of infectious hepatitis C virus in tissue culture from a cloned viral genome. Nat Med 2005;11:791-796.
10. Garaigorta U, Heim MH, Boyd B, Wieland S, Chisari FV. Hepatitis C virus (HCV) induces formation of stress granules whose proteins regulate HCV RNA replication and virus assembly and egress. J Virol 2012;86:11043-11056.
11. Bikkavilli RK, Malbon CC. Arginine methylation of G3BP1 in response to Wnt3a regulates beta-catenin mRNA. J Cell Sci 2011;124:2310-2320.
12. Sarasin-Filipowicz M, Oakeley EJ, Duong FH, Christen V, Terracciano L, Filipowicz W, Heim MH. Interferon signaling and treatment outcome in chronic hepatitis C. Proc Natl Acad Sci U S A 2008;105:7034-7039.
13. Chen L, Borozan I, Feld J, Sun J, Tannis LL, Coltescu C, et al. Hepatic gene expression discriminates responders and nonresponders in treatment of chronic hepatitis C viral infection. Gastroenterology 2005;128:1437-1444.
14. Kudo S, Matsuno K, Ezaki T, Ogawa M. A novel migration pathway for rat dendritic cells from the blood: hepatic sinusoids-lymph translocation. J Exp Med 1997;185:777-784.
15. Chen L, Borozan I, Sun J, Guindi M, Fischer S, Feld J, et al. Cell-type specific gene expression signature in liver underlies response to interferon therapy in chronic hepatitis C infection. Gastroenterology 2010;138:1123-1133.e1-3.
16. Askarieh G, Alsio A, Pugnale P, Negro F, Ferrari C, Neumann AU, et al. Systemic and intrahepatic interferon-gamma-inducible protein 10 kDa predicts the first-phase decline in hepatitis C virus RNA and overall viral response to therapy in chronic hepatitis C. HEPATOLOGY 2010;51:1523-1530.
17. Romanowska M, Evans A, Kellock D, Bray SE, McLean K, Donandt S, Foerster J. Wnt5a exhibits layer-specific expression in adult skin, is upregulated in psoriasis, and synergizes with type 1 interferon. PLoS One 2009;4:e5354.
18. Shapira SD, Gat-Viks I, Shum BO, Dricot A, de Grace MM, Wu L, et al. A physical and regulatory map of host-influenza interactions reveals pathways in H1N1 infection. Cell 2009;139:1255-1267.
19. Staal FJ, Luis TC, Tiemessen MM. WNT signalling in the immune system: WNT is spreading its wings. Nat Rev Immunol 2008;8:581-593.

THE JOURNAL OF BIOLOGICAL CHEMISTRY VOL. 289, NO. 1, pp. 335–345, January 3, 2014

Metformin Suppresses Expression of the Selenoprotein P Gene via an AMP-activated Kinase (AMPK)/FoxO3a Pathway in H4IIEC3 Hepatocytes*[S]

Received for publication, May 1, 2013, and in revised form, November 18, 2013 Published, JBC Papers in Press, November 20, 2013, DOI 10.1074/jbc.M113.479386

Hiroaki Takayama,[a] Hirofumi Misu,[a] Hisakazu Iwama,[b] Keita Chikamoto,[a,c] Yoshiro Saito,[d] Koji Murao,[e] Atsushi Teraguchi,[f] Fei Lan,[a] Akihiro Kikuchi,[a] Reina Saito,[a] Natsumi Tajima,[a] Takayoshi Shirasaki,[a,g] Seiichi Matsugo,[h,i] Ken-ichi Miyamoto,[j,k] Shuichi Kaneko,[a] and Toshinari Takamura[a1]

From the [a]Department of Disease Control and Homeostasis, Kanazawa University Graduate School of Medical Sciences, 13-1 Takara-machi, Kanazawa, Ishikawa 920-8641, Japan, the [b]Life Science Research Center, Kagawa University, Ikenobe 1750-1, Miki-cho, Kita-gun, Kagawa 761-0793, Japan, the [c]Division of Natural System, Graduate School of Natural Science and Technology, Kanazawa University, Kakuma-machi, Kanazawa, Ishikawa 920-1192, Japan, the [d]Systems Life Sciences, Department of Medical Life Systems, Faculty of Medical and Life Sciences, Doshisha University, Kyotanabe, Kyoto 610-0394, Japan, the [e]Departments of Advanced Medicine, Kagawa University, Ikenobe 1750-1, Miki-cho, Kita-gun, Kagawa 761-0793, Japan, the [f]Department of Hospital Pharmacy, Kanazawa University, 13-1 Takara-machi, Kanazawa, Ishikawa 920-8641, Japan, the [g]Department of Advanced Medical Technology, Kanazawa University Graduate School of Health Medicine, 13-1 Takara-machi, Kanazawa, Ishikawa 920-8641, Japan, the [h]Division of Material Engineering, Graduate School of Natural Science and Technology, Kanazawa University, Kakuma-machi, Kanazawa, Ishikawa 920-1192, Japan, the [i]Institute of Science and Engineering, Faculty of Natural System, Kanazawa University, Kakuma-machi, Kanazawa, Ishikawa 920-1192, Japan, the [j]Department of Hospital Pharmacy, Kanazawa University Graduate School of Medical Sciences, 13-1 Takara-machi, Kanazawa, Ishikawa 920-8641, Japan, and the [k]Department of Medicinal Informatics, Kanazawa University Graduate School of Medical Sciences, 13-1 Takara-machi, Kanazawa, Ishikawa 920-8641, Japan

Background: The suppression of selenoprotein P production may be a novel therapeutic target for reducing insulin resistance.
Results: Selenoprotein P expression was suppressed by metformin treatment, but co-administration of AMPK inhibitor or FoxO3a siRNA cancelled this suppression.
Conclusion: Metformin suppresses selenoprotein P expression via the AMPK/FoxO3a pathway.
Significance: The AMPK/FoxO3a pathway in the liver may be a therapeutic target for type 2 diabetes.

Selenoprotein P (SeP; encoded by *SEPP1* in humans) is a liver-derived secretory protein that induces insulin resistance in type 2 diabetes. Suppression of SeP might provide a novel therapeutic approach to treating type 2 diabetes, but few drugs that inhibit *SEPP1* expression in hepatocytes have been identified to date. The present findings demonstrate that metformin suppresses *SEPP1* expression by activating AMP-activated kinase (AMPK) and subsequently inactivating FoxO3a in H4IIEC3 hepatocytes. Treatment with metformin reduced *SEPP1* promoter activity in a concentration- and time-dependent manner; this effect was cancelled by co-administration of an AMPK inhibitor. Metformin also suppressed *Sepp1* gene expression in the liver of mice. Computational analysis of transcription factor binding sites conserved among the species resulted in identification of the FoxO-binding site in the metformin-response element of the *SEPP1* promoter. A luciferase reporter assay showed that metformin suppresses Forkhead-response element activity, and a ChIP assay revealed that metformin decreases binding of FoxO3a, a direct target of AMPK, to the *SEPP1* promoter. Transfection with siRNAs for *Foxo3a*, but not for *Foxo1*, cancelled metformin-induced luciferase activity suppression of the metformin-response element of the *SEPP1* promoter. The overexpression of FoxO3a stimulated *SEPP1* promoter activity and rescued the suppressive effect of metformin. Metformin did not affect FoxO3a expression, but it increased its phosphorylation and decreased its nuclear localization. These data provide a novel mechanism of action for metformin involving improvement of systemic insulin sensitivity through the regulation of SeP production and suggest an additional approach to the development of anti-diabetic drugs.

Selenoprotein P (SeP[2]; encoded by *SEPP1* in humans) is a secretory protein produced mainly by the liver (1, 2). SeP contains 10 selenocysteine residues and is known to transport the essential trace element selenium from the liver to the rest of the

* This work was supported by grants-in-aid from the Ministry of Education, Culture, Sports, Science and Technology, Japan (to H. M., T. T., and S. K.) and research grants from Dainippon Sumitomo Pharma (to S. K.) and Takeda Science Foundation (to H. M.).
[S] This article contains supplemental Figs. S1–S5.
[1] To whom correspondence should be addressed: Dept. of Disease Control and Homeostasis, Kanazawa University Graduate School of Medical Science, 13-1 Takara-machi, Kanazawa, Ishikawa 920-8641, Japan. Tel.: 81-76-265-2233; Fax: 81-76-234-4250; E-mail: ttakamura@m-kanazawa.jp.

[2] The abbreviations used are: SeP, selenoprotein P; AMPK, AMP-activated kinase; AICAR, 5-aminoimidazole-4-carboxamide ribonucleotide; compound C, 6-[4-(2-piperidin-1-yl-ethoxy)-phenyl)]-3-pyridin-4-yl-pyrrazolo[1,5-a]-pyrimidine; cGPx, cellular glutathione peroxidase; DN, dominant negative; CA, constitutive active; TFBS, transcription factor binding site; FHRE, forkhead-response element.

body (3, 4). Our laboratory reported recently that SeP functions as a hepatokine that contributes to insulin resistance in type 2 diabetes (5). Using comprehensive gene expression analyses in humans, hepatic gene expression levels of *SEPP1* were found to be positively correlated with the severity of insulin resistance in patients with type 2 diabetes. Moreover, treatment with purified SeP protein impairs insulin signal transduction in both cell culture and animal models. Importantly, the RNA interference-mediated knockdown of SeP improves insulin resistance and hyperglycemia in a mouse model of type 2 diabetes, suggesting that the suppression of SeP production in the liver may be a novel therapeutic target for reducing insulin resistance in type 2 diabetes (5). However, few drugs that inhibit the production of SeP by hepatocytes have been identified to date.

Metformin is widely used as an anti-diabetic drug globally. The primary target of metformin action is the liver, which abundantly expresses organic cation transporter (Oct)-1, a transporter for metformin (6, 7). Adenosine monophosphate-activated protein kinase (AMPK) mediates primarily the glucose-lowering actions of metformin, including the suppression of hepatic gluconeogenesis (8). In contrast, several reports indicate that the oral administration of metformin in humans increases insulin sensitivity in skeletal muscle, increases serum adiponectin, and improves aortic arteriosclerosis (9–11). These reports suggest that orally administered metformin also exerts beneficial actions on tissues other than the liver, in which expression levels of Octs are lower. To date, however, the molecular mechanisms underlying the systemic actions of metformin are not fully understood.

Forkhead box protein O3a (FoxO3a), which belongs to the Forkhead transcription factors of the FoxO subfamily (FoxOs), is reported to be involved in cell cycle arrest (12), apoptosis (13), and the oxidative stress response (14, 15). Recently, Greer *et al.* (16) showed that FoxO3a, but not FoxO1, is directly phosphorylated and activated by AMPK *in vitro*. FoxO3a is reported to positively regulate mitochondria-related genes, such as uncoupling proteins, in mouse embryonic fibroblasts, suggesting that the direct regulation of FoxO3a by AMPK plays a crucial role in the control of the cellular energy balance. The phosphorylation of FoxO3a by AMPK was also identified in C2C12 myotubes (17), aortic vascular endothelial cells (18), and A549 lung cancer cells (19). However, the role of the AMPK/FoxO3a pathway in hepatocytes, an important target of metformin, remains unknown.

We demonstrate here that metformin suppresses *SEPP1* gene expression by activating AMPK and subsequently inactivating FoxO3a in H4IIEC3 hepatocytes. These results suggest a novel mechanism underlying the glucose-lowering action of metformin.

EXPERIMENTAL PROCEDURES

Materials—The antibodies against AMPKα, phospho-AMPKα, FoxO1, FoxO3a, acetylated Lys, and Lamin A/C were purchased from Cell Signaling Technology (Beverly, MA). Antibody against phospho-Ser/Thr/Tyr was purchased from AnaSpec (San Jose, CA). Antibody against GAPDH was purchased from Santa Cruz Biotechnology, Inc. 5-Aminoimidazole-4-carboxamide ribonucleotide (AICAR) and 6-[4-(2-Piperidin-1-yl-ethoxy)-phenyl)]-3-pyridin-4-yl-pyrrazolo [1,5-a]-pyrimidine (compound C) were purchased from Sigma-Aldrich. FoxO3a expression vector was provided from Ajinomoto Pharma (Tokyo, Japan) described before (20). Selenious acid was purchased from WaKo Pure Chemical Industries, Ltd. (Osaka, Japan). Metformin was provided by Dainippon Sumitomo Pharma (Osaka, Japan).

Generation of Plasmid Constructs—The human *SEPP1* promoter region has been described previously (21). Fragments of ~1800 bp from the human *SEPP1* promoter region and the deletion promoter region were amplified by PCR using normal human genomic DNA as a template and the primer pairs shown in Table 1. The PCR product was subcloned into the luciferase reporter gene plasmid pGL3-basic (Promega, Madison, WI) and termed "*SEPP1*-Promoter-Luc," "Mut-A," "Mut-B," "Mut-C," "Mut-D," "Mut-E," "Mut-DΔ1," "Mut-DΔ2," and "Mut-DΔ3." Putative FoxO binding site-deficient vector were generated using QuikChange Lightning site-directed mutagenesis kits (Agilent Technologies, Santa Clara, CA), according to the manufacturer's instructions. All inserts were confirmed by DNA sequencing.

Cell Culture—Studies were performed using the rat hepatoma cell line H4IIEC3 (American Type Culture Collection, Manassas, VA). Cells were cultured in Dulbecco's modified Eagle's medium (DMEM; Invitrogen) and supplemented with 10% fetal bovine serum (Invitrogen), 2 mmol/liter L-glutamine (WaKo Pure Chemical Industries, Ltd.), 100 units/ml penicillin, and 0.1 mg/ml streptomycin (WaKo Pure Chemical Industries, Ltd.). The cells were cultured at 37 °C in a humidified atmosphere containing 5% CO_2.

Measurement of Glutathione Peroxidase Activity—To measure cellular glutathione peroxidase (cGPx) activity, a coupled enzyme assay, which was performed by following the oxidation of NADPH, was used as described previously (22). In brief, cells were cultured with 1) DMEM plus 10% FBS, 2) DMEM plus 10% FBS and 100 nM selenious acid, or 3) DMEM plus 10% FBS and 1000 nM selenious acid at 72 h. Then cells were fractured with homogenate buffer containing 0.25 M sucrose, 50 mM Tris-HCl (pH 7.4), 0.1 mM EDTA, 0.1 mM 2-mercaptoethanol. The assay conditions were as follows for the cGPx assay: 0.1 M phosphate buffer, pH 7.4, 0.2 mM NADPH, 0.5 mM EDTA, 1 mM NaN_3, 2 mM GSH, 1 unit/ml GSH reductase, and 30 μM hydrogen peroxide. The oxidation of NADPH was followed at 340 nm at 37 °C, and units of the enzyme activity were expressed as μmol of NADPH oxidized/min.

Transfection and Luciferase Reporter Gene Assay—H4IIEC3 cells were grown in 24-well plates and transfected with 0.4 μg of plasmid DNA/well together with 1.2 μl of FuGENE6 (Promega). For the luciferase reporter gene assays, 0.4 μg of firefly luciferase promoter construct was co-transfected with 0.01 μg of *Renilla* luciferase control plasmid (pRL-SV40; Promega) and/or 0.05–0.4 μg of plasmids expressing FoxO3a or empty control plasmids, resulting in a total DNA amount of 0.41–0.81 μg/well. 24 h later, cells were treated with the indicated reagents, such as metformin, in DMEM plus 10% FBS for the indicated times. After 48 h, luciferase activities were measured using the Dual Luciferase assay system (Promega), as described previously (20).

TABLE 1
Primers used in cloning

Primer	Description	Sequence
SEPP1-Promoter-Luc		
Forward	hSeP-promoter-F-BglII	ACTAGATCTACAAACCTTTCAGACACTGAGTTG
Reverse	hSeP-promoter-R-NcoI	ACTCCATGGACAACCACTTCCAACGGGCCTGCTT
Mut-A		
Forward	hSeP-promoter-Del-F1-BglII	ACTAGATCTGGGCTGCCTGTCTTTGATTTCACAT
Reverse	hSeP-promoter-R-NcoI	ACTCCATGGACAACCACTTCCAACGGGCCTGCTT
Mut-B		
Forward	hSeP-promoter-Del-F2-BglII	ACTAGATCTTTGTAGTTCCTGCACCTTGTACAAC
Reverse	hSeP-promoter-R-NcoI	ACTCCATGGACAACCACTTCCAACGGGCCTGCTT
Mut-C		
Forward	hSeP-promoter-Del-F3-BglII	ACTAGATCTGCATAGGTCTTCCAGGAAGTACGAC
Reverse	hSeP-promoter-R-NcoI	ACTCCATGGACAACCACTTCCAACGGGCCTGCTT
Mut-D		
Forward	hSeP-promoter-Del-F4-BglII	ACTAGATCTCAAATGTTTTTCCCTGTTATAGTTT
Reverse	hSeP-promoter-R-NcoI	ACTCCATGGACAACCACTTCCAACGGGCCTGCTT
Mut-E		
Forward	hSeP-promoter-F-BglII	ACTAGATCTACAAACCTTTCAGACACTGAGTTG
Reverse	hSeP-promoter-Del-R1-NocI	ACTCCATGGCTGAGCCAGCGAATTATGCTGCTGC
Mut-DΔ1		
Forward	hSeP-promoter-Del-F14-BglII	ACTAGATCTGATTCTAGGGTGACTGAAAAGGATA
Reverse	hSeP-promoter-R-NcoI	ACTCCATGGACAACCACTTCCAACGGGCCTGCTT
Mut-DΔ2		
Forward	hSeP-promoter-Del-F15-BglII	ACTAGATCTATAACAATCAGCTCAGGGGTTTGCT
Reverse	hSeP-promoter-R-NcoI	ACTCCATGGACAACCACTTCCAACGGGCCTGCTT
Mut-DΔ3		
Forward	hSeP-promoter-Del-F16-BglII	ACTAGATCTATAAATATCAGAGTGTGCTGCTGTG
Reverse	hSeP-promoter-R-NcoI	ACTCCATGGACAACCACTTCCAACGGGCCTGCTT
Mut-DΔ2-ΔFoxo A		
Forward	del86–95	GACTATACCTGAGGGGTGAGGGACTATAAATATCAGAGTG
Reverse	del86–95-antisense	CACTCTGATATTTATAGTCCCTCACCCCTCAGGTATAGTC
Mut-DΔ2-ΔFoxo B		
Forward	hSeP-del-Foxo 3-F	GAGGTAAACAACAGGACTAAGAGTGTGCTGCTGTGG
Reverse	hSeP-del-Foxo 3-R	CCACAGCAGCACACTCTTAGTCCTGTTGTTTACCTC

siRNA Transfection in H4IIEC3 Hepatocytes—H4IIEC3 hepatocytes were grown in 24-well plates and transiently transfected with 10 nM small interfering RNA (siRNA) duplex oligonucleotides using 1 μl of Lipofectamine™ RNAiMAX (Invitrogen) by the reverse transfection method according to the manufacturer's instructions. *Foxo1*- and *Foxo3a*-specific siRNAs with the following sequences were synthesized (Thermo Scientific): *Foxo1* A, 5′-GACAGCAAAUCAAGUUAUG-3′ (sense); *Foxo1* B, 5′-UUUGAUAACUGGAGUACAU-3′ (sense); *Foxo3a* A, 5′-GAACGUUGUUGGUUUGAAC-3′ (sense); and *Foxo3a* B, 5′-CGUCAUGGGUCACGACAAG-3′ (sense). Negative control siRNA was also utilized (Thermo Scientific). 24 h after transfection, the cells were treated with metformin for 24 h, followed by the extraction of total RNA.

Adenovirus-mediated Gene Transfer in H4IIEC3 Hepatocytes—Cells were transfected with adenoviruses as described previously (5). Briefly, H4IIEC3 hepatocytes were grown to 90% confluence in 24-well multiplates and transfected with adenoviruses encoding dominant negative (DN) α1 and α2 AMPK, constitutive active (CA) AMPK, or LacZ for 4 h. The cells were incubated with DMEM for 24 h after removing the adenoviruses; total RNA was then extracted.

Quantitative RT-PCR—Total RNA was extracted from cultured H4IIEC3 hepatocytes using a Genelute mammalian total RNA miniprep kit (Sigma). The reverse transcription of 100 ng of total RNA was performed using a high capacity cDNA reverse transcription kit (Invitrogen), according to the manufacturer's instructions. Quantitative RT-PCR was performed using TaqMan probes (ACTB, 4352340E; Foxo1, Rn01494868_m1; Foxo3, Rn01441087_m1; G6pc, Rn00565347_m1; Pck1, Rn01529014_m1; Sepp1, Rn00569905_m1) and the 7900HT fast real-time PCR system (Invitrogen), as described previously (23).

Western Blotting—Treated cells were collected and lysed as described previously (20). Protein samples (10 μg/lane) were subjected to SDS-PAGE and transferred to PVDF membranes using the iBlot Gel Transfer system (Invitrogen). The membranes were blocked, incubated with primary antibody, washed, and incubated with the secondary HRP-labeled antibody. Bands were visualized with the ECL Prime Western blotting Detection System (GE Healthcare) and LAS-3000 (Fujifilm, Tokyo, Japan). A densitometric analysis of blotted membranes was performed using ImageJ software.

Immunoprecipitation—Immunoprecipitation of serine/threonine/tyrosine-phosphorylated proteins or lysine-acetylated proteins was carried out using the Dynabeads protein G immunoprecipitation kit (Invitrogen) according to the manufacturer's instructions. The nuclear and cytoplasmic fractions were extracted using an NE-PER nuclear and cytoplasmic extraction reagent kit (Pierce).

Detection of the Conserved Transcription Factor Binding Sites Using Multiple-genome Alignments—The Ensembl 12-way Enredo-Pecan-Ortheus (EPO) eutherian multiple alignments (12-way EPO alignments) (24, 25) were downloaded. The 12-way EPO was excised to obtain the alignment block corresponding to the human genome coordinates from 10 kb upstream of the coding sequence of *SEPP1*, including the start

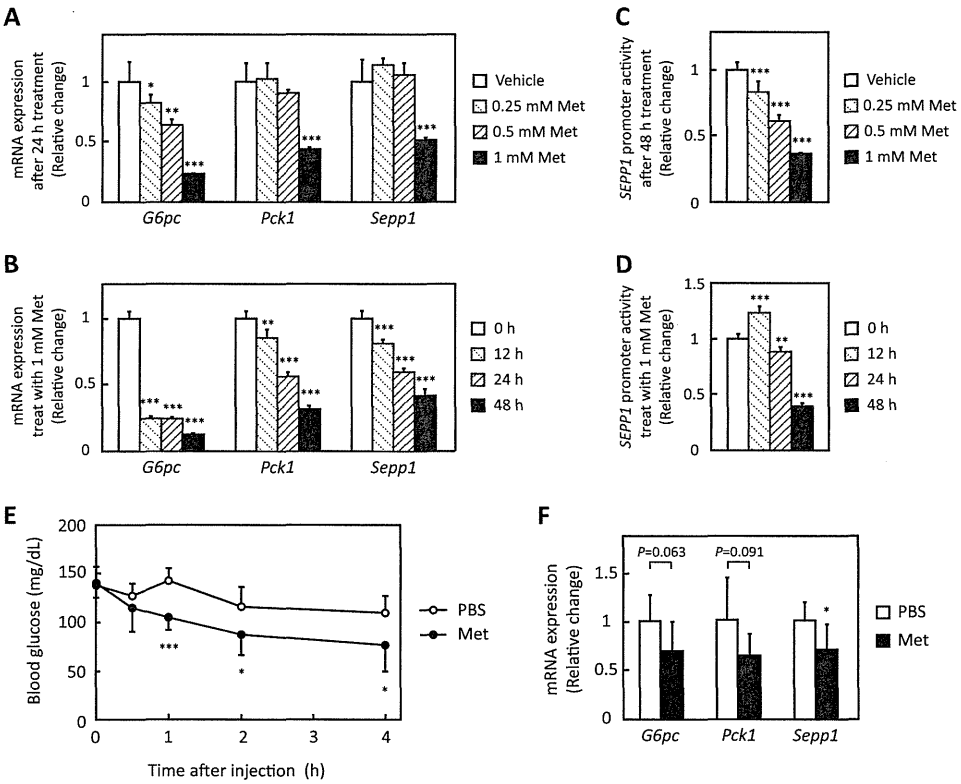

FIGURE 1. **Metformin suppressed *Sepp1* gene expression in H4IIEC3 hepatocytes and livers of C57BL/6J mice.** *A* and *B*, metformin suppressed *Sepp1* mRNA expression in a concentration- and time-dependent manner. H4IIEC3 cells were treated with the indicated concentrations of metformin for the indicated times. Expression values were normalized to *Actb* mRNA. Data represent means ± S.D. (*error bars*) ($n = 4$). *, $p < 0.05$; **, $p < 0.01$; ***, $p < 0.001$ *versus* vehicle-treated cells or 0 h. *C* and *D*, *SEPP1* promoter activity was suppressed in a concentration- and time-dependent manner. H4IIEC3 cells were co-transfected with the *SEPP1* promoter reporter vector and control reporter vector. 24 h later, the cells were treated with the indicated concentrations of metformin for the indicated times. Values were normalized to the activity of the control luciferase vector. Data represent means ± S.D. ($n = 4$). **, $p < 0.01$; ***, $p < 0.001$ *versus* vehicle-treated cells or 0 h. *E* and *F*, metformin suppressed *Sepp1* mRNA expression in livers of C57BL/6J mice. Following fasting for 4 h, 12-week-old female C57BL/6J mice were administrated 300 mg/kg metformin. 4 h after metformin administration, mice were sacrificed, and liver mRNA expression was examined. Expression values were normalized to *Actb* mRNA. Data represent means ± S.D. ($n = 7$). *, $p < 0.05$ *versus* PBS-injected mice.

codon. To predict the conserved transcription factor binding sites (TFBSs), the 10-kb upstream genome sequence for each of the 12 species was searched using the TRANSFAC (26) and the MATCH^{TM} program (27) (version 6.1) with varied thresholds. Then the predicted TFBSs were mapped on the alignments, and the conserved TFBSs for *SEPP1* were identified.

Chromatin Immunoprecipitation (ChIP) Assay—A ChIP assay was carried out using the ChIP IT Express enzymatic kit (Active Motif, Carlsbad, CA) according to the manufacturer's instructions. In brief, HepG2 cells were treated with metformin 6 h before being fixed and homogenized. Following centrifugation, the supernatant was used for chromatin samples. Chromatin samples were incubated with protein G-coated magnetic beads and ChIP grade FoxO1 or FoxO3a antibodies (Abcam, Cambridge, MA) overnight at 4 °C. Following washing and elution, a reaction solution was used as the template for PCR. PCR primers were set for amplification of the Mut-DΔ2 region of the *SEPP1* promoter, as follows: forward, 5′-GCACTTGCTACTTTCTTTTAAGTTG-3′; reverse, 5′-CACAGCAGCACACTCTGATATTTAT-3′.

Animals—12-week-old C57BL/6J female mice were obtained from CLEA Japan, Inc. (Tokyo, Japan). All animals were housed in a 12-h light/dark cycle and allowed free access to food and water. Following the fasting for 4 h, mice were administrated 300 mg/kg metformin. 4 h later, mice were anesthetized and sacrificed to allow isolation of liver tissue.

Statistical Analysis—Results are expressed as means ± S.D. Significance was tested by one-way analysis of variance with the Bonferroni method, and differences were considered statistically significant at a p value of less than 0.05.

RESULTS

Metformin Suppresses SEPP1 Expression at the Promoter Level—The effects of metformin on *Sepp1* expression in H4IIEC3 hepatocytes were examined. Metformin suppressed *Sepp1* mRNA expression in a concentration- and time-dependent manner, similarly to *G6pc* and *Pck1*, which encode representative gluconeogenic enzymes glucose-6-phosphatase and phosphoenolpyruvate carboxykinase 1, respectively (Fig. 1, *A* and *B*). These results are consistent with a previous report using rat primary hepatocytes (28). Next, the effects of metformin on *SEPP1* promoter activity were examined. The human *SEPP1* promoter region was cloned to a luciferase reporter vector as reported previously (21). The present sequence completely corresponded to the reference sequence of the National Center for Biotechnology Information, but it missed one thymidine against the sequence of the previous report (accession number Y12262) (supplemental Fig. S1). Similar to the mRNA results,

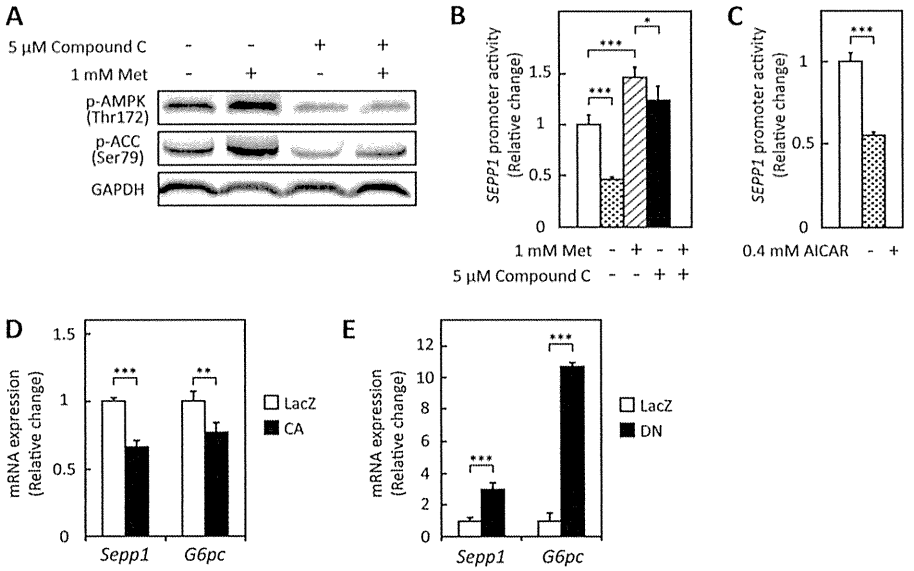

FIGURE 2. **Metformin suppressed *SEPP1* promoter activity via AMPK pathway in H4IIEC3 hepatocytes.** *A*, metformin-induced AMPK phosphorylation in the absence or presence of compound C. H4IIEC3 cells were treated with the indicated concentrations of metformin and compound C for 24 h. AMPK phosphorylation was examined by Western blotting. *B*, compound C treatment recovered metformin-induced suppression of the *SEPP1* promoter. H4IIEC3 cells were co-transfected with the *SEPP1* promoter reporter vector and control reporter vector at 24 h and then treated with the indicated concentrations of metformin and compound C for 48 h. Signals were normalized to the control reporter vector. Data represent means ± S.D. (*error bars*) ($n = 4$). ***, $p < 0.001$. *C*, AICAR suppressed *SEPP1* promoter activity. H4IIEC3 cells were co-transfected with the *SEPP1* promoter reporter vector and control reporter vector at 24 h and then treated with 0.4 mM AICAR for 24 h. Signals were normalized to the control reporter vector. Data represent means ± S.D. ($n = 4$). ***, $p < 0.001$. *D* and *E*, influence of adenoviruses carrying constitutive active (CA) or dominant negative (DN) AMPK. H4IIEC3 cells were infected with adenoviruses encoding CA-AMPK, DN-AMPK, or LacZ. Expression values were normalized to *Actb* mRNA. Data represent means ± S.D. ($n = 4$). **, $p < 0.01$; ***, $p < 0.001$.

metformin suppressed *SEPP1* promoter activity in a concentration- and time-dependent manner (Fig. 1, *C* and *D*), suggesting that it directly decreases *SEPP1* transcriptional activity in H4IIEC3 hepatocytes.

To confirm whether the present experimental condition (DMEM plus 10% FBS) supplied selenium sufficiently to synthesize selenoproteins for cultured cells, cGPx activity was measured with or without additional selenium supplement. Supplemental Fig. S2 indicates that supplementation of 100 or 1000 nM selenious acid to DMEM plus 10% FBS increased cGPx activity more than 3 times, suggesting that our experimental condition was insufficient to maximize selenoprotein synthesis. However, the current activity of cGPx in the cells cultured at DMEM plus 10% FBS (233 units/g) corresponded to the levels reported previously in the normal rat liver tissue (120–1800 units/g) (29, 30). Because these results suggest that the culture condition of DMEM plus 10% FBS was physiological, we used this condition in the following cellular experiments.

The action of metformin on *Sepp1* was also examined in mice. Following fasting for 4 h, 12-week-old female C57BL/6J mice were administrated 300 mg/kg metformin. Metformin decreased blood glucose levels by 30% (Fig. 1*E*) and tended to down-regulate gene expression for *G6pc* and *Pck1* after 4 h. Gene expression of *Sepp1* was significantly decreased by metformin (Fig. 1*F*). These results indicate that metformin suppresses gene expression for *Sepp1* in the liver of mice as well as in the cultured hepatocytes.

Metformin Suppresses SEPP1 Promoter Activity via AMPK Activation—Metformin is known to exert anti-diabetic effects by activating AMPK pathways (31). Hence, to determine whether AMPK pathways are involved in the metformin-induced suppression of *SEPP1* promoter activity, cells were treated with compound C, a representative AMPK inhibitor. Findings confirmed that the metformin-induced phosphorylation of AMPK and acetyl-CoA carboxylase was cancelled by the co-administration of compound C in H4IIEC3 hepatocytes (Fig. 2*A*). Co-administration of compound C partly rescued the cells from the inhibitory effects of metformin on the *SEPP1* promoter (Fig. 2*B*) and increased *SEPP1* promoter activity in the absence of metformin (Fig. 2*B*). In contrast, treatment with AICAR, a known activator of AMPK, decreased *SEPP1* promoter activity similarly to metformin (Fig. 2*C*). To determine whether AMPK pathways were involved in *SEPP1* promoter activity, H4IIEC3 hepatocytes were infected with an adenovirus encoding CA- or DN-AMPK. Transfection with CA-AMPK suppressed *Sepp1* and *G6pc* mRNA expression (Fig. 2*D*), whereas transfection with DN-AMPK enhanced *Sepp1* and *G6pc* mRNA expression (Fig. 2*E*). These results suggest that metformin decreases *SEPP1* promoter activity, at least partly, by activating AMPK.

Metformin-response Element in the SEPP1 Promoter Includes the FoxO Binding Site—To determine the nature of the metformin-response element in the *SEPP1* promoter region, several deletion mutants of the *SEPP1* promoter were constructed (Fig. 3*A*). Promoter activity of Mut-A to Mut-D, but not Mut-E, was suppressed by metformin treatment (Fig. 3*A*), indicating that the metformin-response element of the *SEPP1* promoter exists in Mut-D. Additional deletion mutants of Mut-D were constructed and named Mut-DΔ1 to DΔ3. Mut-DΔ1 and -DΔ2, but not Mut-DΔ3, were suppressed by metformin (Fig. 3*B*), indicating that the metformin-response element in the *SEPP1* promoter is localized in the Mut-DΔ2 sequence. Using computational analysis to identify conserved TFBSs among the species (see "Experimental Procedures"), several putative TFBSs were identified in the Mut-DΔ2 sequence (supplemental Fig. S3).

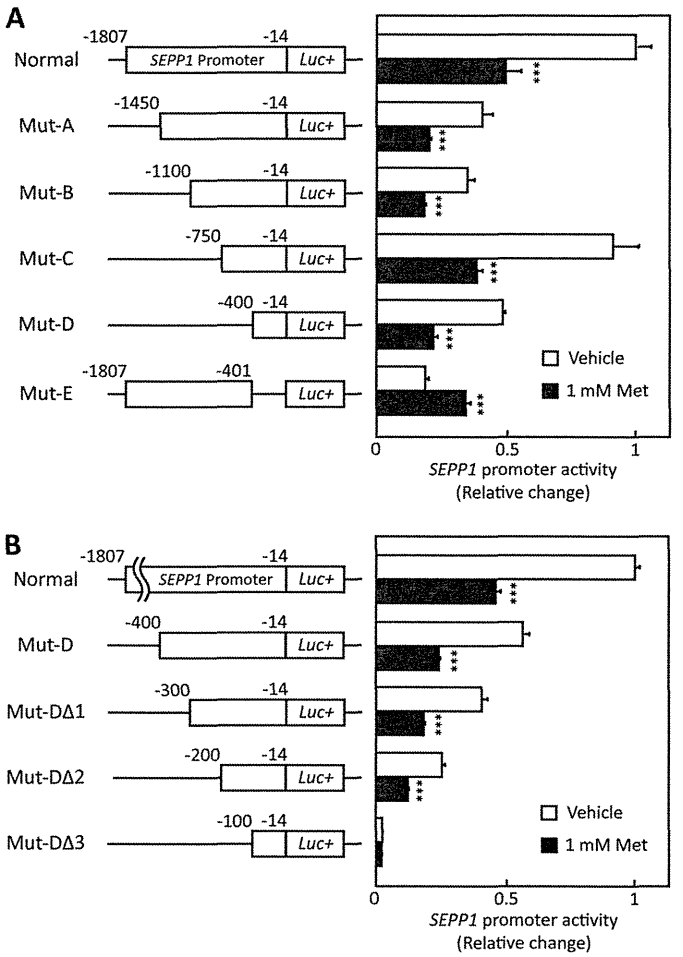

FIGURE 3. **SEPP1 promoter activity of deletion mutants.** *A* and *B*, structure and luciferase activity of promoter-deletion mutants. The sequences deleted within the constructs are shown as *thin lines*. The remaining parts of the *SEPP1* promoter were fused to a luciferase reporter gene. H4IIEC3 cells were co-transfected with each reporter vector and control reporter vector at 24 h and then treated with the indicated concentrations of metformin for 48 h. Signals were normalized to the control reporter vector. Data represent means ± S.D. (*error bars*) ($n = 4$). ***, $p < 0.001$ *versus* vehicle-treated cells.

Because early reports indicate that AMPK directly phosphorylates FoxO3a and regulates its transcriptional activity (16), this investigation focused on the two putative FoxO binding sites (Fig. 4*A*).

Metformin Suppresses FoxO Activity via AMPK Activation—To determine whether metformin treatment influences FoxO activity, a forkhead-response element (FHRE)-Luc vector that includes three tandems of FHREs ligated with a luciferase gene was utilized (32). This vector was used as a reporter of FoxO-responsive promoter activity (33). Metformin treatment suppressed FHRE activity, and concurrent treatment with compound C completely cancelled this suppression (Fig. 4*B*). In addition, treatment with compound C stimulated FHRE activity in the absence of metformin (Fig. 4*B*), whereas AICAR treatment suppressed FHRE activity (Fig. 4*C*). These results suggest that metformin suppresses FHRE activity via AMPK activation. To determine the critical FoxO binding site for metformin-induced *SEPP1* suppression, we constructed luciferase vectors that deleted either of two putative FoxO binding sites and were named Mut-DΔ2-ΔFoxo A or B, respectively (supplemental Fig. S4). Luciferase assay using these vectors revealed that putative FoxO binding site B was essential for metformin-induced *SEPP1* suppression (Fig. 4*D*). Because the assays using these vectors are not specific to FoxO3a activity, the interaction of FoxO proteins with DNA sequences in the *SEPP1* promoter was examined using a ChIP assay. For the ChIP assay, HepG2 cells were utilized to evaluate the human *SEPP1* promoter. Metformin suppressed *SEPP1* expression in HepG2 cells as well as H4IIEC3 cells (data not shown). The ChIP assay indicates that treatment with metformin decreased the binding of FoxO3a to *SEPP1* promoter, whereas it increased the binding of FoxO1 (Fig. 4*E*). These results suggest that FoxO3a, but not FoxO1, is associated with the metformin-induced suppression of *SEPP1* expression.

Metformin Suppresses SEPP1 Expression via FoxO3a Inactivation—Next, we examined whether the specific knockdown of endogenous *Foxo3a* or *Foxo1* affects *Sepp1* expression in H4IIEC3 hepatocytes. Transfection with *Foxo3a*- or *Foxo1*-specific siRNA resulted in a ~50% reduction in mRNA levels of *Foxo3a* or *Foxo1* (Fig. 5*A*). Knockdown of both *Foxo1* and *Foxo3a* resulted in a significant down-regulation of *Sepp1* expression (Fig. 5*A*). Interestingly, mRNA levels of *G6pc* were decreased by *Foxo3a* knockdown (Fig. 5*A*), suggesting that not only FoxO1 but also FoxO3a positively regulates the expression of the gluconeogenesis-related genes in H4IIEC3 hepatocytes. Next, we assessed whether knockdown of *Foxo3a* selectively affects the inhibitory action of metformin on the *SEPP1* promoter. Transfection with siRNAs for *Foxo3a*, but not for *Foxo1*, cancelled metformin-induced suppression of Mut-DΔ2 luciferase activity (Fig. 5*B*). These results suggest that the metformin-induced suppression of *Sepp1* is dependent on FoxO3a but not on FoxO1.

Whether FoxO3a overexpression influences the action of metformin on *SEPP1* promoter activity was also investigated. The FoxO3a protein was overexpressed in a concentration-dependent manner in cells transfected with the pCMV6-FoxO3a expression vector (Fig. 5*C*). Overexpression of FoxO3a significantly enhanced *SEPP1* promoter activity (Fig. 5*D*), and transfection with pCMV6-FoxO3a rescued the cells from the suppressive effect of metformin on *SEPP1* promoter activity in a concentration-dependent manner (Fig. 5, *D* and *E*). These results indicate that metformin decreases *SEPP1* promoter activity and gene expression via FoxO3a inactivation in H4IIEC3 hepatocytes.

Metformin Decreases FoxO3a Protein in the Nuclear Components—To elucidate the mechanism by which metformin inactivates FoxO3a, phosphorylation and acetylation of FoxO3a were examined in hepatocytes treated with metformin. Metformin treatment altered neither mRNA levels of *Foxo3a* (Fig. 6*A*) nor protein levels of FoxO3a (Fig. 6*B*). However, immunoprecipitation experiments revealed that treatment with metformin phosphorylated FoxO3a but not FoxO1 in H4IIEC hepatocytes (Fig. 6, *B* and *C*, and supplemental Fig. S5). Because a previous report indicated that FoxO3a, as well as FoxO1, is deacetylated by sirtuin family proteins downstream of AMPK (34), we examined the deacetylation of FoxO3a and FoxO1. Acetylation of both FoxO1 and FoxO3a was unaffected by metformin administration (Fig. 6, *B* and *C*, and supplemental Fig. S5). To determine the intracellular localization of FoxO3a, the cytosolic and

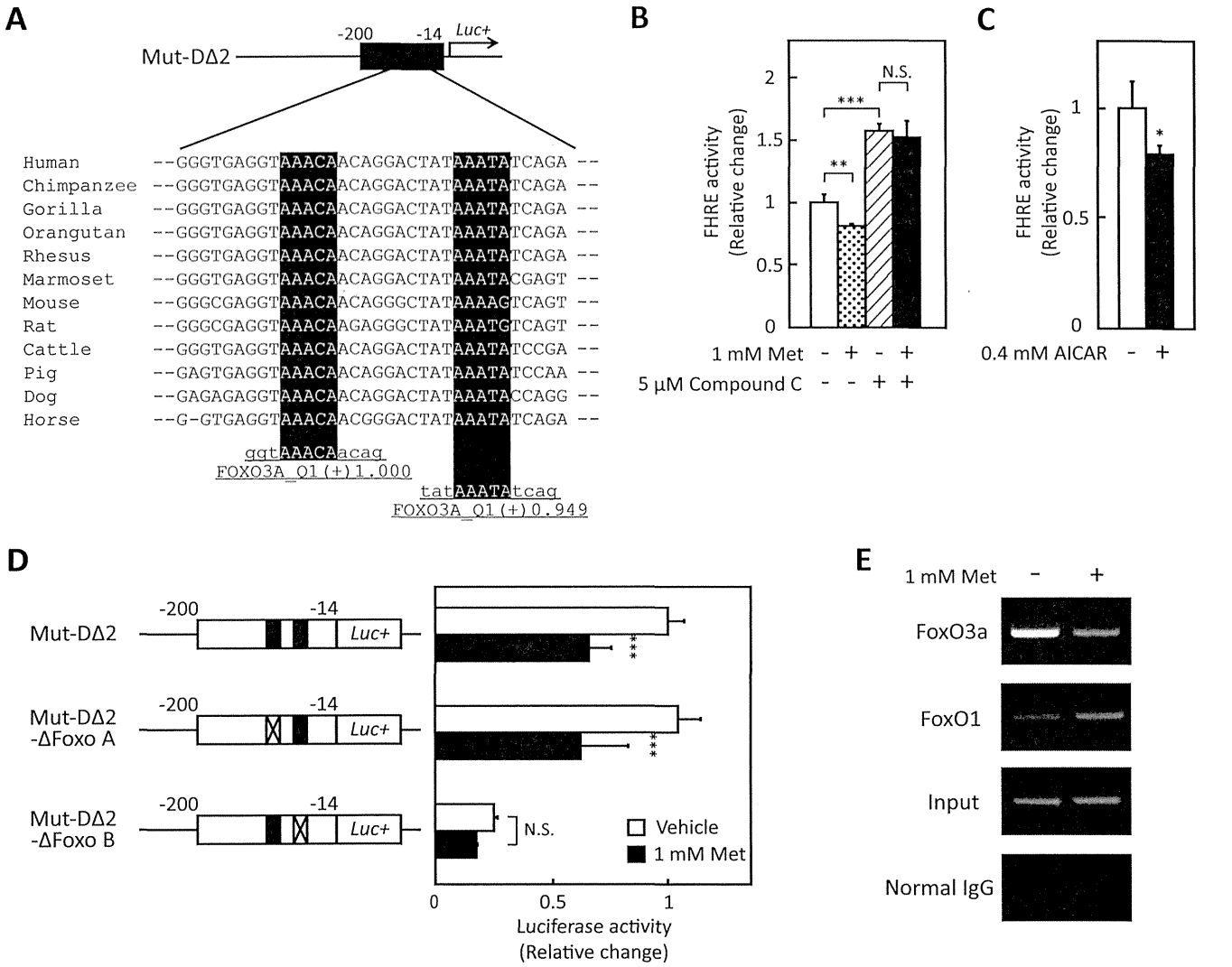

FIGURE 4. **Activation of the AMPK suppressed FoxO activity.** *A*, putative FoxO3a binding sites of Mut-DΔ2 sequence. Detection of the conserved TFBSs was performed using multiple-genome alignments and the *highlighted* putative transcriptional factor binding sites. *B*, FoxO activity in the absence or presence of metformin and compound C. H4IIEC3 cells were co-transfected with the FHRE-Luc vector and control reporter vector at 24 h and then treated with the indicated concentrations of metformin and compound C for 48 h. Signals were normalized to the control reporter vector. Data represent means ± S.D. (*error bars*) ($n = 4$). **, $p < 0.01$; ***, $p < 0.001$. *N.S.*, not significant. *C*, FoxO activity in the absence or presence of AICAR. H4IIEC3 cells were co-transfected with the FHRE-Luc vector and control reporter vector at 24 h and then treated with the indicated concentrations of AICAR for 24 h. Signals were normalized to the control reporter vector. Data represent means ± S.D. ($n = 4$). *, $p < 0.05$ *versus* vehicle-treated cells. *D*, deficiency of putative FoxO binding site cancelled metformin-induced suppression of *SEPP1* promoter activity. H4IIEC3 cells were co-transfected with each reporter vector and control reporter vector at 24 h and then treated with the indicated concentrations of metformin for 24 h. Signals were normalized to the control reporter vector. Data represent means ± S.D. ($n = 4$). ***, $p < 0.001$ *versus* vehicle-treated cells. *E*, chromatin immunoprecipitation assay of HepG2 cells treated with metformin. HepG2 cells were treated with metformin for 6 h. Chromatin samples precipitated with anti-FoxO3a, anti-FoxO1, or normal IgG were amplified using primers for the Mut-DΔ2 region of the human *SEPP1* promoter.

nuclear components of the FoxO3a protein were fractionated. FoxO3a and FoxO1 protein levels were decreased by metformin treatment in the nuclear fraction (Fig. 6*D*). These results suggest that metformin inactivates FoxO3a by decreasing FoxO3a protein levels in the nucleus and subsequently inhibiting the binding of FoxO3a to the *SEPP1* promoter.

DISCUSSION

Our data demonstrate that metformin suppresses production of the insulin resistance-inducing hepatokine SeP by activating AMPK and subsequently inactivating FoxO3a in H4IIEC3 hepatocytes. During the course of this study, it was reported that metformin decreases mRNA levels of *Sepp1* in rat primary hepatocytes (28); however, the molecular mechanisms by which metformin reduces the expression of *Sepp1* were not fully understood. Our data demonstrate that the AMPK/FoxO3a pathway downstream of metformin action plays a major role in the regulation of *SEPP1* expression in cultured hepatocytes. Our data suggest a previously unrecognized mechanism of action of metformin in combating the systemic insulin resistance in type 2 diabetes.

The finding that FoxO3a positively regulates *Sepp1* and *G6pc* expression in H4IIEC3 hepatocytes supports the suggestion that FoxO3a plays an important role in glucose homeostasis. The ability of FoxO1 to increase the expression of gluconeogenic genes has been confirmed (35). To date, however, little

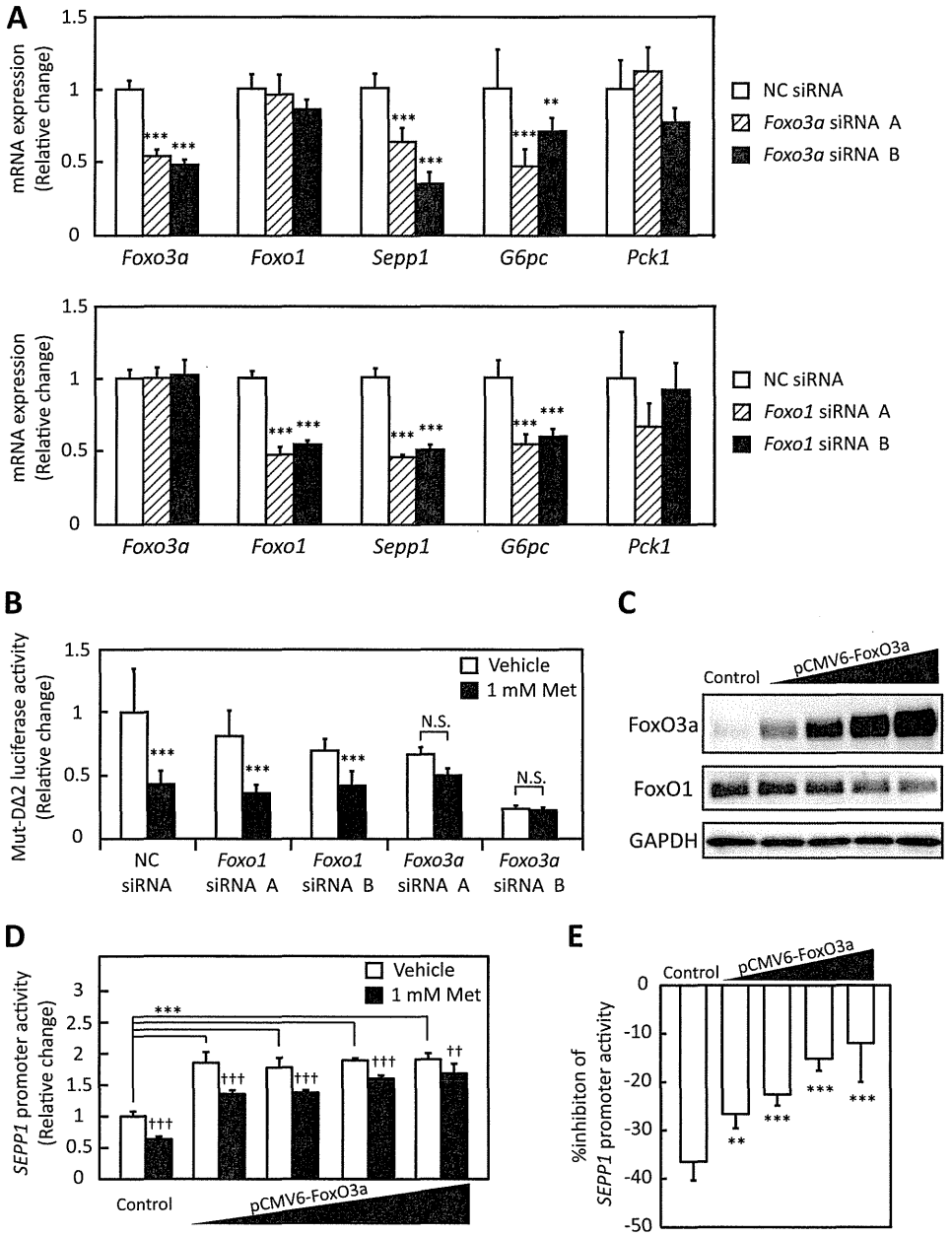

FIGURE 5. **Metformin suppressed SeP expression via FoxO3a.** *A*, efficiency of *Foxo3a* siRNA and *Foxo1* siRNA. H4IIEC3 cells were transfected with *Foxo3a* siRNAs or *Foxo1* siRNAs or a negative control (*NC*) siRNA at 48 h. Knockdown efficiency was assessed by real-time PCR. Expression values were normalized to *Actb* mRNA. Data represent means ± S.D. (*error bars*) ($n = 4$). **, $p < 0.01$; ***, $p < 0.001$ *versus* negative control siRNA-treated cells. *B*, luciferase activity of Mut-DΔ2 treated with *Foxo3a* or *Foxo1* siRNA and metformin. H4IIEC3 cells were transfected with *Foxo3a* siRNAs or *Foxo1* siRNAs or negative control siRNA at 24 h and then co-transfected with Mut-DΔ2 vector and control reporter vector. 24 h after transfection, cells were treated with the indicated concentrations of metformin for 24 h. Signals were normalized to the control reporter vector. Data represent means ± S.D. ($n = 4$). ***, $p < 0.001$ *versus* vehicle-treated cells. *N.S.*, not significant. *C*, protein levels in the presence of the FoxO3a overexpression vector. H4IIEC3 cells were transfected with the pCMV-FoxO3a vector or pCMV empty vector at 24 h. FoxO3a protein levels were then assessed by Western blotting. *D*, *SEPP1* promoter activity transfected with the FoxO3a overexpression vector. H4IIEC3 cells were co-transfected with the expression vectors for FoxO3a, *SEPP1* promoter reporter and control reporter at 24 h and then treated with the indicated concentrations of metformin for 48 h. Data represent means ± S.D. ($n = 3$–4). ***, $p < 0.001$ *versus* control; ††, $p < 0.01$; †††, $p < 0.001$ *versus* vehicle-treated cells. *E*, percentage inhibition of *SEPP1* promoter activity by metformin. Suppression ratios of *SEPP1* promoter activity were calculated based on the data in *E*. Data represent means ± S.D. ($n = 3$–4). **, $p < 0.01$; ***, $p < 0.001$ *versus* control.

information concerning the involvement of FoxO3a in glucose metabolism is available. Certainly, no defects in glucose metabolism have been described in FoxO3a-deficient mice (36), suggesting that the function of FoxO3a in glucose metabolism is compensated for by FoxO1. Indeed, Haeusler *et al.* (37) reported that triple liver-specific ablation of FoxO1, FoxO3a, and FoxO4 causes a more pronounced hypoglycemia and increased insulin sensitivity in mice compared with a single knockout of FoxO1. The present findings indicate that FoxO proteins, including FoxO3a, regulate hepatic glucose metabolism in a coordinated manner. These data reveal that FoxO3a, the downstream target of metformin/AMPK, positively regulates *SEPP1* transcriptional activity in cultured hepatocytes independently of FoxO1 and suggest that

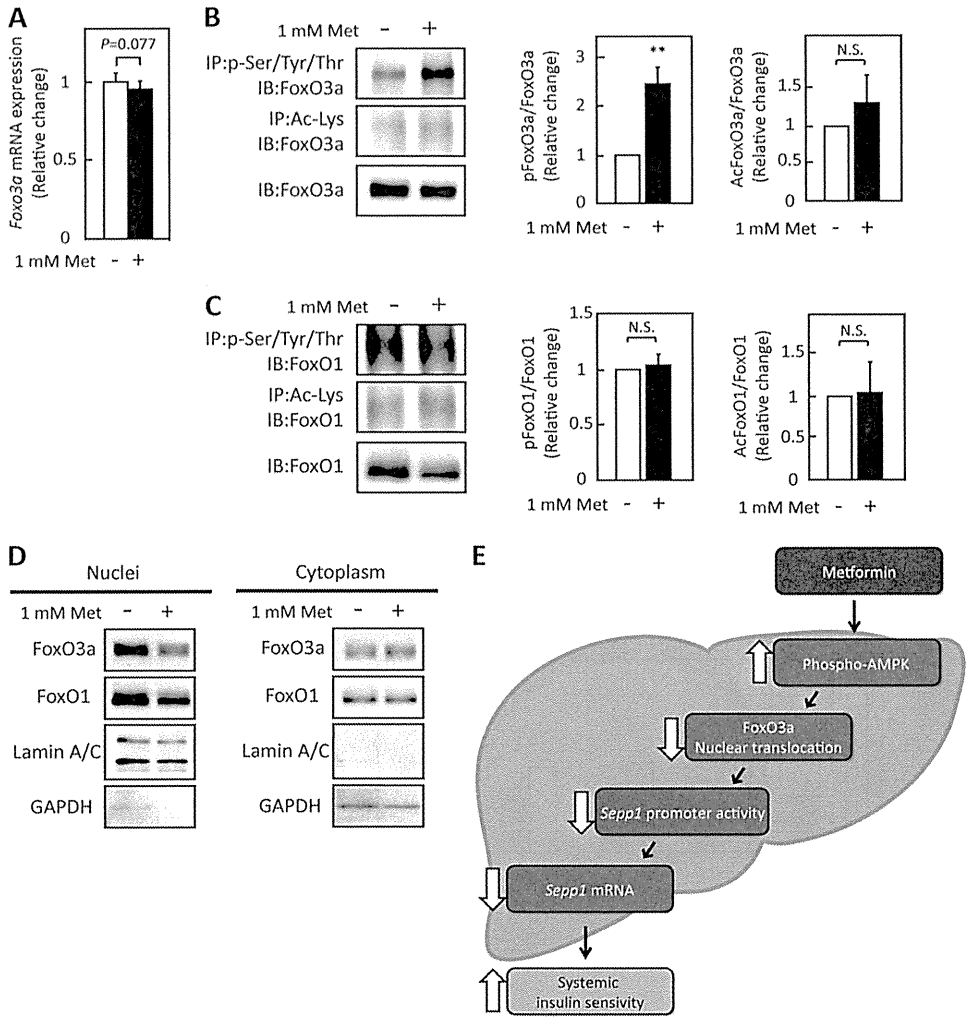

FIGURE 6. **Metformin treatment did not suppress FoxO3a expression but did suppress its activity.** *A*, *FoxO3a* mRNA expression in H4IIEC3 hepatocytes treated with metformin for 6 h. Expression values were normalized to *Actb* mRNA. Data represent means ± S.D. ($n = 5–6$). *B and C*, modification of FoxOs proteins by metformin treatment. Proteins were extracted after 6 h of metformin treatment. Immunoblotting was performed using anti-FoxO3a antibody (*B*) or anti-FoxO1 antibody (*C*). Data represent means ± S.D. ($n = 3$). **, $p < 0.01$. *N.S.*, not significant. *IP*, immunoprecipitation; *IB*, immunoblot. *D*, intracellular localization of FoxO3a and FoxO1 in H4IIEC3 hepatocytes upon treatment with metformin. Proteins were extracted after 6 h of metformin treatment. *E*, scheme of SeP suppression by metformin in the liver. FoxO3a positively regulates *SEPP1* promoter activity. Metformin suppresses FoxO3a activity via AMPK activation, resulting in suppression of SeP expression. Thus, the hypoglycemic effects of metformin may be mediated at least in part by SeP suppression in the liver.

FoxO3a participates in glucose homeostasis via regulation of the hepatic production of SeP, an insulin resistance-inducing hepatokine.

Knockdown of *Foxo3a*, but not *Foxo1*, rescued the cells from metformin-induced inactivation of the *SEPP1* promoter, although knockdown of both *Foxo3a* and *Foxo1* down-regulated *Sepp1* in the absence of metformin (Fig. 5, *A* and *B*). These results are in harmony with early reports showing that FoxO1 positively regulates *Sepp1* expression in cultured hepatocytes (38, 39). The current data suggest that both FoxO3a and FoxO1 positively regulate expression of *SEPP1* in the basal conditions, but FoxO3a has a dominant role in the suppression of *SEPP1* downstream of metformin/AMPK pathway in H4IIEC3 hepatocytes. Interestingly, metformin selectively phosphorylated and deacetylated FoxO3a but not FoxO1 (Fig. 6, *B* and *C*). This FoxO3a-selective phosphorylation by metformin is consistent with the previous report showing that AMPK-induced phosphorylation displays a strong preference toward FoxO3 compared with FoxO1 by using *in vitro* kinase assays (16).

The current study is the first to demonstrate the decreased nuclear localization and subsequent transcriptional inactivation of FoxO3a by AMPK downstream of metformin in the cultured hepatocytes. Greer *et al.* (16) identified FoxO3a as a direct phosphorylation target of AMPK using *in vitro* kinase assays. However, the authors reported that phosphorylation by AMPK increases FoxO3a transcriptional activity without affecting FOXO3A subcellular localization in mouse embryonic fibroblasts or 293T cells. A similar activation of FoxO3a by AMPK was reported in C2C12 myotubes (17). In this respect, our results suggest that the AMPK-induced inactivation of FoxO3a is hepatocyte-specific. When FoxO proteins are phosphorylated by Akt, the dissociation of nuclear co-factors from FoxO is thought to be required for nuclear exclusion of FoxO (40). Hence, the difference in nuclear co-activator/co-repressor

recruitment between hepatocytes and other cells might explain differences in the action of AMPK on FoxO3a cellular localization and transcriptional activity. Notably, the siRNA-induced knockdown of *Foxo3a* decreased *Sepp1* and *G6pc* mRNA levels in H4IIEC3 hepatocytes, suggesting that the AMPK/FoxO3a pathway in the liver regulates gluconeogenesis and the production of the hepatokine SeP. These findings shed light on a previously unrecognized role for the AMPK/FoxO3a pathway in the regulation of glucose metabolism in the liver.

The cancellation of the metformin-induced suppression of SeP by compound C, a known inhibitor of the AMPK pathway, was only partial (Fig. 2*B*). Likewise, the overexpression of FoxO3a only partially cancelled the suppressive action of metformin on *Sepp1* gene expression (Fig. 6, *D* and *E*). These results suggest that metformin decreases *Sepp1* gene expression through both AMPK/FoxO3a-dependent and other independent pathways. Recently, Kalender *et al.* (41) reported that metformin acts to suppress mTORC1 signaling in an AMPK-independent manner. In addition, Guigas *et al.* (42) found that metformin inhibits glucose phosphorylation in primary cultured hepatocytes independently of AMPK activity. Additional studies are needed to elucidate the AMPK-independent actions of metformin on *Sepp1* expression in H4IIEC3 hepatocytes.

The present sequence of *SEPP1* promoter completely corresponds to the refseq of the National Center for Biotechnology Information, but it misses one thymidine against the sequence of a previous report (21). This site had been reported as an SNP site (reference SNP ID rs201851607). Because both allele origin and minor allele frequency of this SNP site are not available, it is difficult to prove which genome sequence is "correct." At least this SNP site does not seem to affect basal *SEPP1* promoter activity. In addition, the metformin-responsible element identified in the current paper locates in the other region of the SNP site. Thus, we consider that the effect of this SNP on the conclusion of this paper is negligible.

A limitation of the present study is that the effects of metformin on SeP expression were not investigated in human samples. The metformin concentrations used in this study (0.25–1 mM) were higher than the blood levels of metformin in patients treated with conventional doses of the drug (10–40 μM). However, it has been pointed out that concentrations of metformin in liver tissue are much higher than those in the blood because the liver receives portal vein blood, which may contain materially higher doses of metformin than plasma (43). An early report indicated that metformin concentrations in the liver were greater than 250 μmol/kg in an STZ diabetic mouse model treated with 50 mg/kg metformin (44). One previous study used 0.25–1 mM metformin in rat primary hepatocytes as a more physiological range of intrahepatic concentration (43). In addition, we show that administration of 300 mg/kg metformin was effective on hepatic expression for *Sepp1* in C57BL/6J mice (Fig. 1*F*). Although clinical trials are necessary, we speculate here that treatment with metformin decreases blood levels of SeP in patients with diabetes. Additionally, the contribution of SeP suppression to the anti-diabetic actions of metformin should be confirmed by additional investigations using *Sepp1*-knock-out mice.

In summary, the present data provide a novel mechanism of action for metformin involving improvement of systemic insulin sensitivity via the regulation of SeP production (Fig. 6*E*) and suggest that AMPK/FoxO3a pathway in the liver may be a therapeutic target to the development of new anti-diabetic drugs.

Acknowledgments—We thank Dr. Atsushi Hirao (Kanazawa University) for providing a vector for FHRE-Luc and Maki Wakabayashi (Kanazawa University) for technical assistance. We thank Fabienne Foufelle (Université Pierre et Marie Curie) for providing adenovirus vector encoding DN-AMPK. We thank In-kyu Lee (Kyungpook National University) for providing adenovirus vector encoding CA-AMPK.

REFERENCES

1. Burk, R. F., and Hill, K. E. (2005) Selenoprotein P. An extracellular protein with unique physical characteristics and a role in selenium homeostasis. *Annu. Rev. Nutr.* **25,** 215–235
2. Carlson, B. A., Novoselov, S. V., Kumaraswamy, E., Lee, B. J., Anver, M. R., Gladyshev, V. N., and Hatfield, D. L. (2004) Specific excision of the selenocysteine tRNA[Ser]Sec (Trsp) gene in mouse liver demonstrates an essential role of selenoproteins in liver function. *J. Biol. Chem.* **279,** 8011–8017
3. Schomburg, L., Schweizer, U., Holtmann, B., Flohé, L., Sendtner, M., and Köhrle, J. (2003) Gene disruption discloses role of selenoprotein P in selenium delivery to target tissues. *Biochem. J.* **370,** 397–402
4. Hill, K. E., Zhou, J., McMahan, W. J., Motley, A. K., Atkins, J. F., Gesteland, R. F., and Burk, R. F. (2003) Deletion of selenoprotein P alters distribution of selenium in the mouse. *J. Biol. Chem.* **278,** 13640–13646
5. Misu, H., Takamura, T., Takayama, H., Hayashi, H., Matsuzawa-Nagata, N., Kurita, S., Ishikura, K., Ando, H., Takeshita, Y., Ota, T., Sakurai, M., Yamashita, T., Mizukoshi, E., Yamashita, T., Honda, M., Miyamoto, K., Kubota, T., Kubota, N., Kadowaki, T., Kim, H.-J., Lee, I., Minokoshi, Y., Saito, Y., Takahashi, K., Yamada, Y., Takakura, N., and Kaneko, S. (2010) A liver-derived secretory protein, selenoprotein P, causes insulin resistance. *Cell Metab.* **12,** 483–495
6. Wang, D.-S., Jonker, J. W., Kato, Y., Kusuhara, H., Schinkel, A. H., and Sugiyama, Y. (2002) Involvement of organic cation transporter 1 in hepatic and intestinal distribution of metformin. *J. Pharmacol. Exp. Ther.* **302,** 510–515
7. Shu, Y., Sheardown, S. A., Brown, C., Owen, R. P., Zhang, S., Castro, R. A., Ianculescu, A. G., Yue, L., Lo, J. C., Burchard, E. G., Brett, C. M., and Giacomini, K. M. (2007) Effect of genetic variation in the organic cation transporter 1 (OCT1) on metformin action. *J. Clin. Invest.* **117,** 1422–1431
8. Boyle, J. G., Salt, I. P., and McKay, G. A. (2010) Metformin action on AMP-activated protein kinase. A translational research approach to understanding a potential new therapeutic target. *Diabet. Med.* **27,** 1097–1106
9. Malin, S. K., Gerber, R., Chipkin, S. R., and Braun, B. (2012) Independent and combined effects of exercise training and metformin on insulin sensitivity in individuals with prediabetes. *Diabetes Care* **35,** 131–136
10. Singh, S., Akhtar, N., and Ahmad, J. (2012) Plasma adiponectin levels in women with polycystic ovary syndrome. Impact of Metformin treatment in a case-control study. *Diabetes Metab. Syndr.* **6,** 207–211
11. Shargorodsky, M., Omelchenko, E., Matas, Z., Boaz, M., and Gavish, D. (2012) Relation between augmentation index and adiponectin during one-year metformin treatment for nonalcoholic steatohepatosis. Effects beyond glucose lowering? *Cardiovasc. Diabetol.* **11,** 61
12. Medema, R. H., Kops, G. J., Bos, J. L., and Burgering, B. M. (2000) AFX-like Forkhead transcription factors mediate cell-cycle regulation by Ras and PKB through p27kip1. *Nature* **404,** 782–787
13. Luo, X., Puig, O., Hyun, J., Bohmann, D., and Jasper, H. (2007) Foxo and Fos regulate the decision between cell death and survival in response to UV irradiation. *EMBO J.* **26,** 380–390
14. Kops, G. J., Dansen, T. B., Polderman, P. E., Saarloos, I., Wirtz, K. W., Coffer, P. J., Huang, T.-T., Bos, J. L., Medema, R. H., and Burgering, B. M.

(2002) Forkhead transcription factor FOXO3a protects quiescent cells from oxidative stress. *Nature* **419,** 316–321
15. Olmos, Y., Valle, I., Borniquel, S., Tierrez, A., Soria, E., Lamas, S., and Monsalve, M. (2009) Mutual dependence of Foxo3a and PGC-1α in the induction of oxidative stress genes. *J. Biol. Chem.* **284,** 14476–14484
16. Greer, E. L., Oskoui, P. R., Banko, M. R., Maniar, J. M., Gygi, M. P., Gygi, S. P., and Brunet, A. (2007) The energy sensor AMP-activated protein kinase directly regulates the mammalian FOXO3 transcription factor. *J. Biol. Chem.* **282,** 30107–30119
17. Sanchez, A. M., Csibi, A., Raibon, A., Cornille, K., Gay, S., Bernardi, H., and Candau, R. (2012) AMPK promotes skeletal muscle autophagy through activation of forkhead FoxO3a and interaction with Ulk1. *J. Cell Biochem.* **113,** 695–710
18. Li, X.-N., Song, J., Zhang, L., LeMaire, S. A., Hou, X., Zhang, C., Coselli, J. S., Chen, L., Wang, X. L., Zhang, Y., and Shen, Y. H. (2009) Activation of the AMPK-FOXO3 pathway reduces fatty acid-induced increase in intracellular reactive oxygen species by upregulating thioredoxin. *Diabetes* **58,** 2246–2257
19. Lützner, N., Kalbacher, H., Krones-Herzig, A., and Rösl, F. (2012) FOXO3 is a glucocorticoid receptor target and regulates LKB1 and its own expression based on cellular AMP levels via a positive autoregulatory loop. *PLoS One* **7,** e42166
20. Honda, M., Takehana, K., Sakai, A., Tagata, Y., Shirasaki, T., Nishitani, S., Muramatsu, T., Yamashita, T., Nakamoto, Y., Mizukoshi, E., Sakai, Y., Yamashita, T., Nakamura, M., Shimakami, T., Yi, M., Lemon, S. M., Suzuki, T., Wakita, T., and Kaneko, S. (2011) Malnutrition impairs interferon signaling through mTOR and FoxO pathways in patients with chronic hepatitis C. *Gastroenterology* **141,** 128–140, 140.e1–140.e2
21. Dreher, I., Jakobs, T. C., and Köhrle, J. (1997) Cloning and characterization of the human selenoprotein P promoter. Response of selenoprotein P expression to cytokines in liver cells. *J. Biol. Chem.* **272,** 29364–29371
22. Takebe, G., Yarimizu, J., Saito, Y., Hayashi, T., Nakamura, H., Yodoi, J., Nagasawa, S., and Takahashi, K. (2002) A comparative study on the hydroperoxide and thiol specificity of the glutathione peroxidase family and selenoprotein P. *J. Biol. Chem.* **277,** 41254–41258
23. Nakamura, S., Takamura, T., Matsuzawa-Nagata, N., Takayama, H., Misu, H., Noda, H., Nabemoto, S., Kurita, S., Ota, T., Ando, H., Miyamoto, K., and Kaneko, S. (2009) Palmitate induces insulin resistance in H4IIEC3 hepatocytes through reactive oxygen species produced by mitochondria. *J. Biol. Chem.* **284,** 14809–14818
24. Flicek, P., Amode, M. R., Barrell, D., Beal, K., Brent, S., Carvalho-Silva, D., Clapham, P., Coates, G., Fairley, S., Fitzgerald, S., Gil, L., Gordon, L., Hendrix, M., Hourlier, T., Johnson, N., Kähäri, A. K., Keefe, D., Keenan, S., Kinsella, R., Komorowska, M., Koscielny, G., Kulesha, E., Larsson, P., Longden, I., McLaren, W., Muffato, M., Overduin, B., Pignatelli, M., Pritchard, B., Riat, H. S., Ritchie, G. R., Ruffier, M., Schuster, M., Sobral, D., Tang, Y. A., Taylor, K., Trevanion, S., Vandrovcova, J., White, S., Wilson, M., Wilder, S. P., Aken, B. L., Birney, E., Cunningham, F., Dunham, I., Durbin, R., Fernández-Suarez, X. M., Harrow, J., Herrero, J., Hubbard, T. J., Parker, A., Proctor, G., Spudich, G., Vogel, J., Yates, A., Zadissa, A., and Searle, S. M. (2012) Ensembl 2012. *Nucleic Acids Res.* **40,** D84–D90
25. Paten, B., Herrero, J., Beal, K., Fitzgerald, S., and Birney, E. (2008) Enredo and Pecan. Genome-wide mammalian consistency-based multiple alignment with paralogs. *Genome Res.* **18,** 1814–1828
26. Wingender, E. (2008) The TRANSFAC project as an example of framework technology that supports the analysis of genomic regulation. *Brief. Bioinform.* **9,** 326–332
27. Kel, A. E., Gössling, E., Reuter, I., Cheremushkin, E., Kel-Margoulis, O. V., and Wingender, E. (2003) MATCH. A tool for searching transcription factor binding sites in DNA sequences. *Nucleic Acids Res.* **31,** 3576–3579
28. Speckmann, B., Sies, H., and Steinbrenner, H. (2009) Attenuation of hepatic expression and secretion of selenoprotein P by metformin. *Biochem. Biophys. Res. Commun.* **387,** 158–163
29. Łukaszewicz-Hussain, A., and Moniuszko-Jakoniuk, J. (2004) Liver catalase, glutathione peroxidase, and reductase activity, reduced glutathione and hydrogen peroxide levels in acute intoxication with chlorfenvinphos, an organophosphate insecticide. *Pol. J. Environ. Stud.* **13,** 303–309
30. Magwere, T., Naik, Y. S., and Hasler, J. A. (1997) Effects of chloroquine treatment on antioxidant enzymes in rat liver and kidney. *Free Radic. Biol. Med.* **22,** 321–327
31. Zhou, G., Myers, R., Li, Y., Chen, Y., Shen, X., Fenyk-Melody, J., Wu, M., Ventre, J., Doebber, T., Fujii, N., Musi, N., Hirshman, M. F., Goodyear, L. J., and Moller, D. E. (2001) Role of AMP-activated protein kinase in mechanism of metformin action. *J. Clin. Invest.* **108,** 1167–1174
32. Brunet, A., Bonni, A., Zigmond, M. J., Lin, M. Z., Juo, P., Hu, L. S., Anderson, M. J., Arden, K. C., Blenis, J., and Greenberg, M. E. (1999) Akt promotes cell survival by phosphorylating and inhibiting a Forkhead transcription factor. *Cell* **96,** 857–868
33. Eckers, A., Sauerbier, E., Anwar-Mohamed, A., Hamann, I., Esser, C., Schroeder, P., El-Kadi, A. O., and Klotz, L.-O. (2011) Detection of a functional xenobiotic response element in a widely employed FoxO-responsive reporter construct. *Arch. Biochem. Biophys.* **516,** 138–145
34. Cantó, C., Gerhart-Hines, Z., Feige, J. N., Lagouge, M., Noriega, L., Milne, J. C., Elliott, P. J., Puigserver, P., and Auwerx, J. (2009) AMPK regulates energy expenditure by modulating NAD^+ metabolism and SIRT1 activity. *Nature* **458,** 1056–1060
35. Puigserver, P., Rhee, J., Donovan, J., Walkey, C. J., Yoon, J. C., Oriente, F., Kitamura, Y., Altomonte, J., Dong, H., Accili, D., and Spiegelman, B. M. (2003) Insulin-regulated hepatic gluconeogenesis through FOXO1-PGC-1α interaction. *Nature* **423,** 550–555
36. Hosaka, T., Biggs, W. H., 3rd, Tieu, D., Boyer, A. D., Varki, N. M., Cavenee, W. K., and Arden, K. C. (2004) Disruption of forkhead transcription factor (FOXO) family members in mice reveals their functional diversification. *Proc. Natl. Acad. Sci. U.S.A.* **101,** 2975–2980
37. Haeusler, R. A., Kaestner, K. H., and Accili, D. (2010) FoxOs function synergistically to promote glucose production. *J. Biol. Chem.* **285,** 35245–35248
38. Speckmann, B., Walter, P. L., Alili, L., Reinehr, R., Sies, H., Klotz, L.-O., and Steinbrenner, H. (2008) Selenoprotein P expression is controlled through interaction of the coactivator PGC-1α with FoxO1a and hepatocyte nuclear factor 4α transcription factors. *Hepatology* **48,** 1998–2006
39. Walter, P. L., Steinbrenner, H., Barthel, A., and Klotz, L.-O. (2008) Stimulation of selenoprotein P promoter activity in hepatoma cells by FoxO1a transcription factor. *Biochem. Biophys. Res. Commun.* **365,** 316–321
40. Van Der Heide, L. P., Hoekman, M. F., and Smidt, M. P. (2004) The ins and outs of FoxO shuttling. Mechanisms of FoxO translocation and transcriptional regulation. *Biochem. J.* **380,** 297–309
41. Kalender, A., Selvaraj, A., Kim, S. Y., Gulati, P., Brûlé, S., Viollet, B., Kemp, B. E., Bardeesy, N., Dennis, P., Schlager, J. J., Marette, A., Kozma, S. C., and Thomas, G. (2010) Metformin, independent of AMPK, inhibits mTORC1 in a rag GTPase-dependent manner. *Cell Metab.* **11,** 390–401
42. Guigas, B., Bertrand, L., Taleux, N., Foretz, M., Wiernsperger, N., Vertommen, D., Andreelli, F., Viollet, B., and Hue, L. (2006) 5-Aminoimidazole-4-carboxamide-1-β-D-ribofuranoside and metformin inhibit hepatic glucose phosphorylation by an AMP-activated protein kinase-independent effect on glucokinase translocation. *Diabetes* **55,** 865–874
43. Foretz, M., Hébrard, S., Leclerc, J., Zarrinpashneh, E., Soty, M., Mithieux, G., Sakamoto, K., Andreelli, F., and Viollet, B. (2010) Metformin inhibits hepatic gluconeogenesis in mice independently of the LKB1/AMPK pathway via a decrease in hepatic energy state. *J. Clin. Invest.* **120,** 2355–2369
44. Wilcock, C., and Bailey, C. J. (1994) Accumulation of metformin by tissues of the normal and diabetic mouse. *Xenobiotica* **24,** 49–57